American Mineralogist, Volume 76, pages 1408–1425, 1991

The remarkable långbanite structure type: Crystal structure, chemical crystallography, and relation to some other cation close-packed structures

Paul Brian Moore
Department of the Geophysical Sciences, The University of Chicago, Chicago, Illinois 60637, U.S.A.
Pradip K. Sen Gupta
Department of Geology, Memphis State University, Memphis, Tennessee 38152, U.S.A.
Yvon Le Page
National Research Council, Ottawa, Ontario K1A 0R6, Canada

Abstract

Långbanite, which is trigonal polar with $a = 11.563(2)$, $c = 11.100(2)$ Å, space group $P31m$, $Z = 3$, end-member formula $Mn^{2+}_4Mn^{3+}_3Sb^{5+}Si^{4+}_2O_{24}$, has 33 unique atoms in the asymmetric unit, 13 of which are cations and 20 of which are anions. This extraordinary structure is based on "double hexagonal" close packing of cations in the sequence ·ABAC· ≡ ·ch·; $R = 0.065$ for 3654 unique reflections.

In långbanite, no polyhedral faces are shared, but 45.5% (240) of the 528 edges in the unit cell are shared. As a result of cation-cation repulsion, these are among the shortest edges for their respective polyhedra. Polyhedral distance averages are $^{[6]}Sb^{5+}$-O 1.99, $^{[6]}M(1)^{2+}$-O 2.30, $^{[6]}M(2)^{2+}$-O 2.23, $^{[8]}C(5)^{2+}$-O 2.32, $^{[5]}M(6)^{3+}$-O 1.98, $^{[6]}M(3)^{3+}$-O 2.04, $^{[6]}M(4)^{3+}$-O 2.03, $^{[6]}M(7)^{3+}$-O 2.04, $^{[6]}M(8)^{3+}$-O 2.03, $^{[6]}M(9)^{3+}$-O 2.07, $^{[4]}Si(1)$-O 1.63, $^{[4]}Si(2)$-O 1.62, and $^{[4]}Si(3)$-O 1.56 Å, with M principally $Mn_{0.89}Fe_{0.11}$.

Unlike the cations, the anion arrangement is not based on principles of close packing. The structure is conceived as consisting of four discrete layers which link by corner and edge sharing. At $z = 0$, the $^2_\infty[Mn^{2+}_9Sb^{5+}_3O_{24}]$ ordered brucite-like sheet has a $^2_\infty[M^{2+}_3O_8]$ unit that mimics the octahedral sheet of spinel along [111]. At $z = ¼$, the $^2_\infty[Mn^{3+}_9O_6(SiO_4)(SiO_4)_2O_{18}]$ unit relates to a sheet in schairerite, $Na_{21}(SO_4)_7F_6Cl$, and to the fundamental $^2_\infty[Fe^{3+}_9O_6(PO_4)(PO_4)_2(PO_4)_6]$ sheet in mitridatite. At $z = ½$, the $^2_\infty[Mn^{2+}_3O_6Mn^{3+}_9O_{33}]$ sheet relates to pyrochlore and the large alunite-jarosite family. At $z = ¾$, the $^2_\infty[Mn^{3+}_9O_3(SiO_4)_3O_{18}O_3]$ sheet is based on $Mn^{3+}_3OO_{12}$ islands of three Mn^{3+}–O atom distorted octahedra comprising three shared edges and one shared vertex, all nearly in a plane. This highly strained sheet mimics the sheets in the important cement phase alite, Ca_3OSiO_4.

The difference Δ (Å) between positions of atoms of långbanite's sheet at $z = ¼$ and those of the related sheet in schairerite is 0.48 Å (mean); in mitridatite, it is 0.39 Å (mean). These values apply to centroids of all atoms in these related sheets. Transforming the cell of lanthanum to one with $a' = 2\sqrt{3}a = 13.06$ and $c = 12.16$ Å, $c/a' = 0.931$, 48 La, all 13 unique cations in långbanite can be directly compared to invariant atom positions of La. The difference is $\Delta = 0.17$ Å (range 0.04–0.33 Å). Långbanite is considered to be an oxide-stuffed version of the La intermetallic structure.

Five independent $Mn^{3+}O_6$ octahedra exhibit pronounced $4d^4$ Mn^{3+} Jahn-Teller distortion. The average Mn^{3+}-O distances are 1.94 (four equatorial) and 2.27 Å (two apical). The *extrema* for individual distances of these five polyhedra are 1.87 and 2.39 Å.

Introduction

Few exotic mineral species have engendered more confusion and discussion in the literature than långbanite. The sporadic but persistent appearance as an early skarn mineral of the iron manganese oxide ores in dolomitic marbles from the Bergslagen district, Värmland province, central Sweden, and the presence of at least ten components in six earlier chemical analyses that involve five valence states among transition metals opened the floodgates of speculation. Långbanite was originally named and described by Flink (1887), and ensuing studies afforded a great diversity of proposed formulae. Oxidation state was the principal problem. The only conclusions that could be reached placed the phase somewhere in the system CaO-MnO-FeO-Mn_2O_3-Fe_2O_3-Y_2O_3-Sb_2O_3-SiO_2-MnO_2-Sb_2O_5.

The literature on långbanite is extensive, and only the

0003–004X/91/0708–1408$02.00

more definitive investigations will be emphasized. A key monograph by Magnusson (1930) is the most thorough treatise on the Långban (formerly Långbanshyttan) deposits to date. Långbanite is discussed in some detail, and Magnusson placed it among the earliest Mn-skarn minerals, where it crystallized with rhodonite, "schefferite," and hedyphane. He listed six earlier analyses (number of independent analyses in parentheses after component weight percent): H_2O 0.32 wt% (1); MgO 0.40–1.61 (5); CaO 1.73–2.98 (5); MnO 66.29 (1), 31.54–36.82 (5); FeO 10.32 (1); Fe_2O_3 3.44–14.31 (5); Sb_2O_3 11.61–15.35 (5); SiO_2 8.75–12.23 (6); MnO_2 26.15–35.15 (5); and Sb_2O_5 15.42 (1). Clearly, this hodgepodge of cation oxides suggests a formidable chemical crystallographic problem. Our plan, therefore, was to obtain electron probe analyses for a långbanite crystal and to submit a portion of the same crystal to X-ray single crystal structure analysis. Knowledge of the elements present and a refined crystal structure would admit proper apportioning of cations and their appropriate valences over the asymmetric unit.

Moore (1970) proposed an end-member formula for långbanite: $Mn^{2+}_4Mn^{3+}_9Sb^{5+}Si^{4+}_2O_{24}$, with $Z = 3$. Although this formula seemed to resolve many contradictions, no cell contents are valid without further evidence, in this case structure analysis. Actually, Moore began structure analysis as early as 1964, but over the years many new trials and data sets met with failure. The best convergence led to $R \sim 0.16$. Space groups tested included $P\bar{3}1m$ and $P31m$, the latter shown to be correct in this study. Rau and Kurkutova (1973) claimed to have solved the structure of långbanite, but their structure was based on the subcell $a' = a/\sqrt{3}$ and $R = 0.17$. In addition, they proposed, among other polyhedra, $Mn^{4+}O_6$ octahedra and $Mn^{3+}O_5$ trigonal bipyramids. Our study contravenes their proposed structure. The chemical crystallographic relations and drafting of this manuscript were effected by Moore (P.B.M.), the data measurement and solution by Le Page (Y.L.), and the structure refinement by Sen Gupta (P.K.S.).

The structure of långbanite represents an extreme case of homometricity. A remarkable paper by Strunz (1944) presaged the intricate chemical crystallography of långbanite, bixbyite, and braunite. His cell transform was a serendipitous clue to the genealogy of långbanite. Långbanite is also related to the complex mineral schairerite, $3Na_{21}S_7O_{28}F_6Cl$, the structure of which was solved by Fanfani et al. (1975), a feat in structure solution; probably to tranquillityite, $6Fe^{2+}_8Zr_2Ti^{4+}_3Si_3O_{24}$, a lunar phase described by Lovering et al. (1971); to the sheet in alite, Ca_3OSiO_4, of Jeffery (1952); and to the sheet in mitridatite, $Ca_6(H_2O)_6[Fe^{3+}_9O_6(PO_4)_3(PO_4)_6]\cdot 3H_2O$, of Moore and Araki (1977). This cornucopia of crystal structures possesses all 13 cations in its asymmetric unit with positions that are within 0.3 Å of centroids in the La (Ce, Nd, Am, Bk, etc.) structure type, which is based on ·ch· "double hexagonal" close-packing of cations. Conversely, långbanite O anions do not display any resemblance to any sensible close packing.

Långbanite: experimental details

Chemical relations

Because the chemical crystallography of långbanite has such a long and contradictory history, we placed the cart before the horse and solved the crystal structure first, and then investigated chemical contents through electron probe analysis. This proved to be a boon, for we were able to assess valence states on the basis of bond distances and coordination polyhedra.

The chemical analysis was straightforward and appears as oxides in Table 1. No evidence of H_2O molecules could be found by Penfield tube determination, and the compound was assumed to be anhydrous. An average of eight independent analyses revealed six elements besides O in quantity greater than 0.05 wt%. The cations were assumed to be Ca^{2+}, Y^{3+}, Fe^{3+}, and Sb^{5+}, with Mn of undetermined average formal charge. On the basis of 24 O atoms and 16 cations in the formula unit, a valence balance equation could be written with only one variable. The solution for a formula unit ($Z = 3$) is, in order of decreasing Pauling radii for cations,

$$Ca^{2+}_{0.26}Y^{3+}_{0.01}Mn^{2+}_{4.00}Mn^{3+}_{7.23}Fe^{3+}_{1.38}Sb^{5+}_{1.15}Si^{4+}_{1.97}O_{24.00}.$$

On the basis of the refined crystal structure analysis, cations are grouped accordingly:

$$^{[8]}(Mn^{2+}_{0.73}Ca^{2+}_{0.26}Y^{3+}_{0.01})_{\Sigma=1.00} \qquad ^{[6]}Mn^{2+}_{3.00}$$

$$^{[6]}(Mn^{3+}_{6.23}Fe^{3+}_{1.38}Mn^{2+}_{0.27}Sb^{5+}_{0.15})_{\Sigma=8.03} \qquad ^{[6]}Sb^{5+}_{1.00}$$

$$^{[5]}Mn^{3+}_{1.00} \qquad ^{[4]}Si^{4+}_{1.97}O_{24.00}.$$

Computation of density gives $D(\text{calc}) = 4.97$ g cm^{-3}; this compares favorably with $D(\text{obs}) = 4.9$ of Ramdohr and Strunz (1980) and $D(\text{obs}) = 4.92$ of Flink (1887).

The formula shows anion coordination numbers about cations of 8, 6, 5, and 4. The formulas above support the end-member formula $Mn^{2+}_4Mn^{3+}_9Sb^{5+}Si^{4+}_2O_{24}$ suggested by

Table 1. Långbanite chemical analysis

Component	Weight percent 1	2
MnO	21.96	22.24
CaO	1.11	—
Y_2O_3	0.06	—
Fe_2O_3	8.56	—
Mn_2O_3	44.21	55.66
SiO_2	9.14	9.42
Sb_2O_5	14.36	12.68
Total	99.40	100.00

Note: Column 1 is oxide weight percent, elements with Z greater than that of O from Cameca microprobe analysis, 15 kV accelerating voltage, 25 nA current, wavelength dispersive spectrum (energy dispersive spectrum for check), I.M. Steele, operator. The standards were: Si, diopside (wt. frac. 0.2594); Y, YAG (wt. frac. 0.4493); Ca, diopside (wt. frac. 0.1851); Sb, Sb_2S_3 (wt. frac. 0.7172); Fe, manganese hortonolite (wt. frac. 0.3439); Mn, manganese hortonolite (wt. frac. 0.0397). Column 1 is an average of eight different analyses. Column 2 is oxide weight percent for ideal $Mn^{2+}_4Mn^{3+}_9Sb^{5+}Si^{4+}_2O_{24}$.

TABLE 2. Experimental data for långbanite

Crystal-cell data	
a (Å)	11.563(2)
c (Å)	11.100(2)
V (Å^3)	1285.2(3)
Space group	$P31m$
Z	3
Formula	$Mn_4^{2+}Mn_8^{3+}Sb^{5+}Si_2^{4+}O_{24}$ (end-member)
D(calc) (g cm^{-3})	4.946 (end-member)
μ_l (cm^{-1})	114.8
Intensity measurements	
Crystal size (μm)	180 × 180 × 100 (‖c)
Diffractometer	Enraf-Nonius CAD-4
Monochromator	Graphite
Radiation	Mo$K\alpha$
Scan type	θ-2θ
2θ range	2°–90°
Reflections measured	3696
Unique reflections > $2\sigma(F_o)$	3654 F_o used in refinement
Secondary extinction coefficient	8.5(4) × 10^{-2} Zachariasen (1968)
Refinement of structure	
R 0.065	$R = \Sigma(\|\|F_o\| - \|F_c\|\|)/\Sigma F_o$
R_w 0.059	$R_w = [\Sigma_w(\|F_o\| - \|F_c\|)^2/\Sigma_w F_o^2]^{1/2}$
	$w = \sigma^2(F)$
Variable parameters	211
Goodness of fit (GOF)	2.93

Moore (1970), which shall be the working formula used in this study.

Crystal structure analysis

Earlier attempts, *vide supra,* not only failed to converge with R less than 0.16 but also supported a profound homometric character among the atoms. The only conclusion reached was that the space group was $P31m$.

Y.L. obtained the most recent data and solved the crystal structure. Although ambiguities remain, *vide infra,* the convergence and the bond distance and angle criteria suggest a sensible structure. An outline of experimental data appears in Table 2. The crystal, a squat hexagonal prism, was selected from some crystals of sample U.S. NMNH B-18215. These sharp, lustrous, iron black crystals were supplied by John S. White, Jr., Curator of Minerals, U.S. National Museum. A total of 34 reflections with limits $24° < 2\theta < 36°$ provided the refined unit-cell parameters given in Table 2. All data were corrected for Lorentz and polarization factors and for absorption, the latter based on an empirical ψ scan. Atomic scattering factors for Sb, Mn, Si, and O were obtained from Ibers and Hamilton (1974). A rather large coverage to $2\theta = 90°$ for Mo$K\alpha$ radiation was used, resulting in 3654 independent F_o used in the remainder of the study.

Using a NRC VAX crystal structure program adapted for a Digital 8820 computer, Y.L. deduced the structure by "brute force." A few of the heavier atoms (Sb, Mn) whose positions were earlier determined with some confidence were included with one averaged scattering curve and only variable site population parameters. After several iterations, Sb and Mn were allocated to specific sites. A difference map bootstrapped the process, and with iterations followed by new atom additions, all atoms were located. Individual neutral atom scattering curves were then introduced. The lowest symmetry group, $P31m$, was used, again obviating any initial bias. There was no reason (split reflections, poor merging of equivalent reflections, etc.) to suspect a lower symmetry space group. Such a procedure, helpful for extremely homometric structures, is possible only with the recent advent of very high-speed computers.

When R was reduced to 0.08, refinement was continued by P.K.S., who succeeded in gradually obtaining convergence to $R = 0.065$ with anisotropic temperature factors (Table 2). Bond distances, angles, and polyhedral distortions (e.g., foreshortened shared polyhedral edges) were especially helpful in appraising the correctness of the structure refinement.

Earlier communication of the långbanite study was long delayed following refinement. Although all traditional structure and bonding characters appeared reasonable, some thermal vibration parameters were either nonpositive-definite or unreasonably large. This is especially apparent for atom centroids at level $z \sim 3/4$. Note that such thermal parameters (see below) are considerably dilated (oblate) in the (001) plane. Many attempts to solve this problem were made: constrained refinement, difference syntheses, and even different arrangements of some atoms, particularly O(15), O(16), O(18), O(19), O(20). All choices of models guided by the difference syntheses led to even worse catastrophes. It was therefore concluded that the sheet at $z = 3/4$ is only partly ordered or is the dominant sheet averaged with at least one other sheet type. We conclude that the långbanite model we present is that of an average structure, a kind of relation which is observed more frequently as more and more complex structures are refined to higher levels of precision. Future reassessment of the structure is certainly warranted, particularly using a tiny sphere of about 1–10 μm radius and a synchrotron or rotating anode X-ray source.

Table 2 outlines experimental details, Table 2a[1] the most recent observed and calculated structure factors, Table 3 refined atomic coordinates, and Table 3a the anisotropic thermal parameters. Table 4 lists the bond distances and angles; because the distances are largely arrayed according to increasing values, most shared edges appear as the first and shortest O-O distances for their polyhedra. Caution must be exercised, however, as high spin d^4 Mn^{3+} is a Jahn-Teller ion with valence electrons remaining and its coordination polyhedron is intrinsically distorted.

LÅNGBANITE: CHEMICAL CRYSTALLOGRAPHIC RELATIONS

Overview of structure

Despite the fact that långbanite has a relatively small cell ($V = 1285.2$ Å^3), most of the atoms are in special positions in polar space group $P31m$. In fact, 33 atoms occur in the asymmetric unit of which 13 are cations (total

[1] A copy of Table 2a may be ordered as Document AM-91-467 from the Business Office, Mineralogical Society of America, 1130 Seventeenth Street NW, Suite 330, Washington, DC 20036, U.S.A. Please remit $5.00 in advance for the microfiche.

TABLE 3. Långbanite atomic coordinate parameters

	Atom	*R*	*x*	*y*	*z*		La		Δ (Å)
$z = 0$	M(1)	3	0.8312(3)	0	0.9950(5)	5/6	0	0	0.06
	M(2)	6	0.5002(2)	0.3284(1)	0.9878(2)	3/6	2/6	0	0.15
	Sb	3	0.34355(5)	0	0.99100(fixed)	2/6	0	0	0.16
	O(1)	1	0	0	0.0776(16)				
	O(2)	2	2/3	1/3	0.0812(10)				
	O(3)	3	0.4947(7)	0	0.0821(9)				
	O(4)	6	0.3458(6)	0.1449(7)	0.0850(6)				
	O(5)	3	0.1923(10)	0	0.9015(9)				
	O(6)	3	0.6696(8)	0	0.8975(11)				
	O(7)	6	0.4879(7)	0.1489(8)	0.8960(6)				
$z = 1/4$	M(3)	3	0.5272(1)	0	0.2561(2)	3/6	0	1/4	0.32
	M(4)	6	0.3297(1)	0.1550(1)	0.2593(1)	2/6	1/6	1/4	0.16
	Si(1)	1	0	0	0.2286(5)	0	0	1/4	0.23
	Si(2)	2	2/3	1/3	0.2319(5)	4/6	2/6	1/4	0.20
	O(8)	3	0.1317(6)	0	0.2792(7)				
	O(9)	3	0.3587(6)	0	0.2887(6)				
	O(10)	3	0.6996(7)	0	0.2259(8)				
	O(11)	3	0.5441(7)	0	0.4348(9)				
	O(12)	6	0.5342(5)	0.3291(6)	0.2821(5)				
	O(13)	6	0.3252(6)	0.1841(6)	0.4355(6)				
$z = 1/2$	C(5)	3	0.3396(1)	0	0.4922(3)	2/6	0	1/2	0.12
	M(6)	3	0.8363(2)	0	0.4995(3)	5/6	0	1/2	0.04
	M(7)	6	0.4948(1)	0.3252(1)	0.4862(2)	3/6	2/6	1/2	0.18
	O(14)	3	0.1388(10)	0	0.5605(9)				
	O(15)	3	0.3308(19)	0	0.6921(13)				
	O(16)	3	0.7946(29)	0	0.7031(23)				
	O(17)	6	0.5293(7)	0.1929(7)	0.5424(7)				
	O(18)	6	0.4419(27)	0.3127(31)	0.6940(17)				
$z = 3/4$	M(8)	3	0.1670(3)	0	0.7324(2)	1/6	0	3/4	0.20
	M(9)	6	0.5041(2)	0.1674(2)	0.7212(2)	3/6	1/6	3/4	0.33
	Si(3)	3	0.6680(3)	0	0.7529(4)	4/6	0	3/4	0.04
	O(19)	2	2/3	1/3	0.7551(14)				
	O(20)	1	0	0	0.7749(29)				
								Average	0.17 Å
								Range	0.04–0.33 Å

Note: Atoms in långbanite arranged according to level along [001]. Level, atom designation, equipoint rank (*R*), fractional coordinates (*x*, *y*, *z*), invariant La positions (La) and difference between långbanite and La positions (Δ, Å computed from långbanite cell) complete the columns. Standard errors in parentheses refer to the last digit.

of 48 cations in the unit cell) and 20 are anions (total of 72 anions in the unit cell) (see Table 3). In this study, we use M as a symbol for five- and sixfold-coordinated cations and C for the eightfold-coordinated cation. In our crystal M and C are principally $Mn_{0.89}Fe_{0.11}$, and selective partitioning of Fe^{3+} is suggested later. In many respects, this large number of unique atoms hindered a much earlier solution to the crystal structure, and it was only through a new analytical technique that Y.L. succeeded in solving the structure. A description of the profound homometricity, especially noted among the cations, will conclude this section, where it is shown that all cations mimic the atomic positions of La to a remarkable degree. In addition, it will be shown that the långbanite structure is based on the double hexagonal close-packed arrangement of cations, ·ch· in condensed nomenclature or ·ABAC· in atom stacking nomenclature along [001].

The structure, albeit complex, can be conceived as the interlamination of four discrete layers of cations coordinated by anions. As extensive corner and edge sharing occurs between these layers, each individual cation layer has associated anions that frequently are also bonded to an adjacent cation layer. Therefore, each layer is described by first listing cations and their associated anions. The remarkable feature is that in this way, each layer is shown to be represented in other structure types such that the whole edifice of four layers describes many structure types already known. The entire ensemble, in effect, embraces a large number of fundamental building blocks (fbb) and modules of other structure types. This number appears to be enormous and suggests that långbanite, perhaps more than any other structure type, points to the root of structure type and fbb among minerals. Although this very complex structure has been solved, sections of its arrangement will be found to be common to other structures in the future. In fact, Moore and Araki (1977) presaged the present study by asserting its relationship to that of the complex mineral mitridatite, $Ca_6(H_2O)_6[Fe^{3+}_9O_6(PO_4)(PO_4)_2(PO_4)_6]\cdot 3H_2O$, that has 75 atoms in the asymmetric unit. The unit in brackets of the mitridatite formula corresponds to one of the layers in långbanite. Here, in this layer and in the others, we compare an individual layer to that of långbanite through appropriate cell transformation if necessary. The relationship calculated will be a difference in atom position, that is, Δ (Å) = |A − B|(T) where A = långbanite atomic coordinates, B = atomic coordinates suitably transformed for the other structure type being compared, and T corresponds to långbanite

TABLE 3A. Långbanite anisotropic and equivalent isotropic thermal-vibration parameters ($\times 10^2$)

	U_{11}	U_{22}	U_{33}	U_{12}	U_{13}	U_{23}	B(eq), Å^2
M(1)	1.67(7)	U_{11}	4.31(15)	1.17(8)	1.29(8)	U_{13}	1.90(8)
M(2)	0.88(4)	0.66(3)	1.30(4)	0.39(3)	−0.16(3)	−0.02(4)	0.75(3)
Sb	0.72(2)	U_{11}	0.60(2)	0.28(2)	−0.09(2)	U_{13}	0.57(1)
O(1)	1.5(3)	U_{11}	0.8(5)	½ U_{11}	0	0	1.0(3)
O(2)	0.6(2)	U_{11}	0.3(3)	½ U_{11}	0	0	0.4(2)
O(3)	0.6(2)	U_{11}	1.0(3)	−0.3(2)	0.0(2)	U_{13}	0.8(2)
O(4)	0.9(2)	1.1(2)	1.3(2)	0.7(2)	0.1(2)	−0.1(2)	0.8(2)
O(5)	1.8(3)	U_{11}	1.2(3)	0.7(3)	0.0(2)	U_{13}	1.3(3)
O(6)	1.5(3)	U_{11}	1.4(4)	0.8(3)	−0.1(2)	U_{13}	1.1(3)
O(7)	1.2(2)	1.5(2)	0.6(2)	0.7(2)	0.2(2)	−0.1(2)	0.9(2)
M(3)	−0.02(2)	U_{11}	0.62(4)	−0.23(3)	−0.05(3)	U_{13}	0.23(3)
M(4)	0.62(3)	0.09(3)	0.55(3)	0.30(2)	0.04(3)	0.09(3)	0.29(3)
Si(1)	0.8(1)	U_{11}	0.4(2)	½ U_{11}	0	0	0.5(1)
Si(2)	0.4(1)	U_{11}	1.8(2)	½ U_{11}	0	0	0.7(1)
O(8)	0.7(2)	U_{11}	1.2(3)	0.2(2)	0.4(2)	U_{13}	0.7(2)
O(9)	0.0(1)	U_{11}	0.3(2)	−0.1(1)	−0.0(1)	U_{13}	0.2(3)
O(10)	0.4(2)	U_{11}	1.6(3)	0.5(2)	0.5(2)	U_{13}	0.5(2)
O(11)	0.3(1)	U_{11}	1.6(3)	0.1(2)	−0.1(2)	U_{13}	0.6(2)
O(12)	0.5(2)	1.0(2)	0.3(1)	0.5(1)	0.3(1)	−0.1(1)	0.4(1)
O(13)	0.6(2)	0.7(2)	1.1(2)	0.2(1)	−0.1(1)	0.0(1)	0.7(2)
C(5)	1.14(4)	U_{11}	0.86(4)	0.7(5)	0.0(5)	U_{13}	0.78(4)
M(6)	0.73(4)	U_{11}	1.45(8)	0.4(4)	0.2(4)	U_{13}	0.76(5)
M(7)	0.66(3)	0.59(3)	0.97(4)	0.29(3)	−0.15(3)	−0.07(3)	0.60(3)
O(14)	2.1(3)	U_{11}	0.6(3)	1.1(3)	0.1(2)	U_{13}	1.2(3)
O(15)	5.2(8)	U_{11}	1.5(5)	2.7(9)	−0.8(5)	U_{13}	3.1(7)
O(16)	8.7(14)	U_{11}	4.9(11)	7.2(15)	0.0(10)	U_{13}	4.8(12)
O(17)	1.4(2)	1.0(2)	0.8(2)	0.8(2)	0.3(2)	−0.0(2)	0.8(2)
O(18)	14.8(17)	21.6(23)	4.2(8)	15.2(18)	1.9(10)	2.4(12)	8.5(17)
M(8)	3.43(10)	U_{11}	0.50(6)	2.82(11)	0.05(6)	U_{13}	1.55(8)
M(9)	2.41(7)	2.63(8)	0.81(5)	1.91(6)	0.17(4)	0.19(4)	1.31(6)
Si(3)	0.9(1)	U_{11}	0.6(1)	0.4(1)	−0.1(1)	U_{13}	0.6(1)
O(19)	6.0(8)	U_{11}	0.3(4)	½ U_{11}	0	0	3.3(5)
O(20)	24.2(45)	U_{11}	−1.0(5)	½ U_{11}	0	0	12.5(28)

Note: The U_{ij} values are coefficients in the expression $\exp[-\Sigma_{ij}U_{ij}hh_j]$. Estimated standard errors refer to the last digit, and identities are noted.

cell parameters. We shall see that these differences are relatively small (<1 Å) and that there is a close relationship among these structures.

The four unique layers in långbanite are now considered. The first, at $z = 0$ (Fig. 1a), is an ordered brucite-type layer and embraces a host of structures. The second, at $z = ¼$ (Fig. 1b), corresponds to a layer in mitridatite and a similar sheet in schairerite. The third, at $z = ½$ (Fig. 1c), embraces the enormous pyrochlore family, as well as a sheet of hexagonal tungsten bronze and alunite, jarosite, and their kin. The fourth, at $z = ¾$ (Fig. 1d), rather exotic in appearance, is not rare at all but constitutes the basis of six independent sheets in schairerite and those in the very important phase alite, Ca_3OSiO_4, a principal phase in the cement industry. Beyond these four sheets or modules, an additional host of structure types can be found, created by dissecting or breaking apart the individual sheets.

Description of each of the four sheets could constitute an essay in itself, and one of them (at $z = ¼$) will be singled out for special discussion. At $z = 0$, a brucite-like edge-sharing octahedral sheet is ordered, with $3[Sb^{5+}O_6]$ octahedra and a Kagomé $(6\cdot3\cdot6\cdot3)$ net of $^2_\infty[Mn^{2+}_9O_{24}] \equiv 3^2_\infty[Mn^{2+}_3O_8]$ edge-sharing distorted octahedra, which corresponds to the spinel octahedral sheet normal to [111]. The distortions of the $M(1)O_6$ and $M(2)O_6$ octahedra are similar to each other, *vide infra.*

The $^2_\infty Mn^{3+}_9O_6(SiO_4)(SiO_4)_2O_{18}$ sheet occurs at $z = ¼$. This module shall be extensively discussed, *vide infra.* The $^2_\infty Mn^{2+}_3O_6Mn^{3+}_9O_{33}$ sheet occurs at $z = ½$. Both the $3M(6)^{3+}O_5$ square pyramids and $6M(7)^{3+}O_6$ octahedra corner link in the plane to form a Kagomé $(6\cdot3\cdot6\cdot3)$ net, $^2_\infty[M^{3+}_9O_{33}]$. The next longer distance $M(6)^{3+}$-O(8) = 3.00 Å (×2) is deemed too long for a bond. If the $M(6)O_5$ square pyramid is converted into an octahedron, then the unit $^2_\infty[M^{3+}_9O_{36}]$ is created; it corresponds to the $^2_\infty[M^{3+}\phi_4]$ sheet in the large alunite-jarosite family and with $^2_\infty C^{2+}O_2M^{3+}_3O_{12}$, one of two kinds of sheets normal to [111] of the structure of the large pyrochlore family. The sheet at $z = ½$ in långbanite has fragments that are richly represented in other crystal structures.

The last sheet at $z = ¾$ was a surprise initially. Its composition, $Mn^{3+}_9O_6(SiO_4)_3O_{18} \equiv Mn^{3+}_9O_3(SiO_4)_3O_{18}O_3$, is similar to that of the sheet at $z = ¼$, but the polyhedral arrangement is different. Trigonal trimers of edge-sharing octahedra share three edges and one central vertex (the first O_3 in the sheet formula) and create $[Mn^{3+}_3OO_{12}]$ islands. This cluster further links above and below through O_{18} of the formula and laterally to other trigonal trimers by corner sharing (the second in O_3 in the formula). The

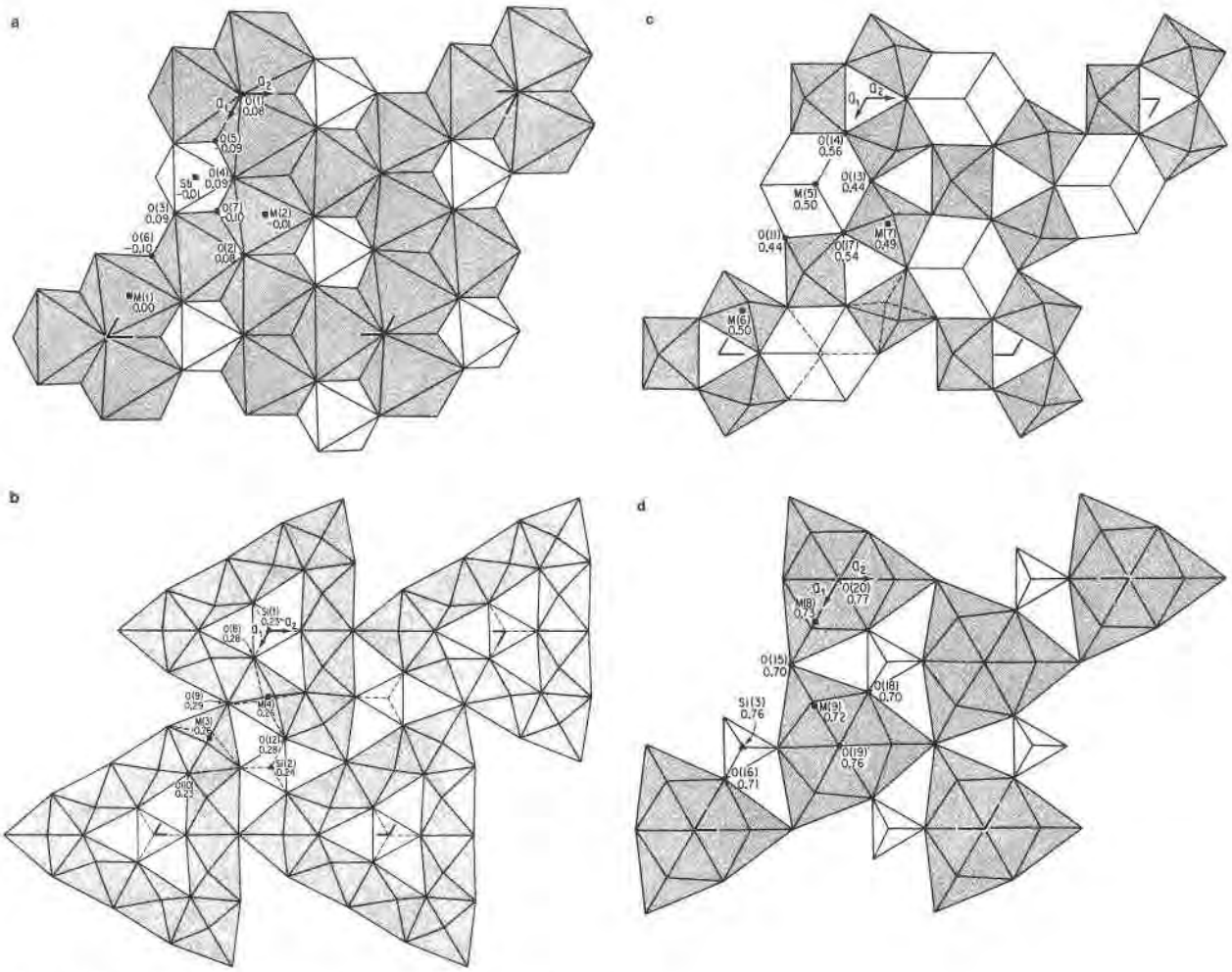

Fig. 1. The långbanite modules are shown at levels $z = 0$, ¼, ½, and ¾. Designated atom positions correspond to Table 3. Key units are stippled. Heights are fractional coordinates in z. (**a**) The långbanite sheet at $z = 0$. The cations Sb, M(1), and M(2) and the anions O(1) through O(7) are labeled. The stippled region corresponds to $\frac{1}{\infty}[M_3O_8]$, the octahedral sheet of spinel along [111]. (**b**) The långbanite sheet at $z = ¼$. The cations Si(1), Si(2), M(3), and M(4) and the anions O(8), O(9), O(10), and O(12) are labeled. Note octahedral edge-sharing nonamers. This sheet is related to units in mitridatite and schairerite. (**c**) The långbanite sheet at $z = ½$. The cations C(5) [≡ M(5)], M(6), and M(7) and the anions O(11), O(13), O(14), and O(17) are labeled. Note stippled sheet, which relates to hexagonal tungsten bronze and the alunite-crandallite families. The entire module is found as one of two sheets of pyrochlore along [111]. (**d**) The långbanite sheet at $z = ¾$. The cations Si(3), M(8), and M(9) and the anions O(15), O(16), O(18), O(19), and O(20) are labeled. Note $Mn_3^{3+}OO_{12}$ islands of edge-sharing octahedra. This module relates to those in schairerite and to alite. This sheet is probably partly disordered.

$(SiO_4)_3$ tetrahedra complete the condensation. As noted earlier, thermal vibration parameters suggest instability for this sheet. The strain induced at the edge-sharing trigonal trimeric islands is considerable. For M(8), the O(16)-O(20)-O(16) angle is 109.9°; for M(9), the O(18)-O(19)-O(18) is 113.3°. For a perfect planar arrangement of octahedral trigonal trimers, the angle would be 120°. However, in both cases, relaxation of strain evidently occurs by movements of the central O(19) and O(20) out of the plane.

Comparison of the $[M_9\phi_6(TO_4)(TO_4)_2O_{18}]$ sheets in långbanite, schairerite, and mitridatite

A remarkable sheet of edge-sharing, octahedral, nonameric rings occurs in långbanite (Fig. 1b), schairerite, and mitridatite. The sheet includes one corner-sharing tetrahedron in the center of the nonameric ring and two other tetrahedra, each of which corner links to three nonamers. Nine octahedra share nine edges to form the trigonal nonamer. All terminal vertices of octahedra and tetrahedra point up or down and associate with adjacent layers.

Table 4. Långbanite polyhedral interatomic distances and angles

$z = 0$		**Sb**	
	2 Sb-O(4)	1.963(8)	
	2 Sb-O(7)	1.997(6)	
	1 Sb-O(5)	2.011(12)	
	1 Sb-O(3)	2.019(8)	
	average	1.992 Å	
			angle (°)
	2 O(4)-O(7)	2.65(1)* **	84.0(3)
	2 O(4)-O(5)	2.67(1)* **	84.4(3)
	2 O(3)-O(7)	2.71(1)* **	85.1(3)
	1 O(4)-O(4)$^{(5)}$	2.90(1)	95.3(3)
	2 O(3)-O(4)	2.94(1)	95.3(4)
	2 O(5)-O(7)	2.96(1)	95.2(3)
	1 O(7)-O(7)$^{(5)}$	2.98(1)	96.6(4)
	average	2.82	90.0
		M(1)	
	1 M(1)-O(1)	2.16(1)	
	1 M(1)-O(6)	2.16(1)	
	2 M(1)-O(5)$^{(1)}$	2.34(1)	
	2 M(1)-O(4)$^{(1)}$	2.41(1)	
	average	2.30	
	2 O(4)$^{(1)}$-O(5)$^{(1)}$	2.67(1)* **	68.3(3)
	2 O(1)-O(5)$^{(1)}$	2.96(2)* **	82.2(3)
	2 O(4)$^{(1)}$-O(6)	3.06(1)* **	83.7(3)
	2 O(5)$^{(1)}$-O(6)	3.32(1)	95.1(4)
	2 O(1)-O(4)$^{(1)}$	3.48(1)	99.0(3)
	1 O(5)$^{(1)}$-O(5)$^{(4)}$	3.85(1)	110.5(4)
	1 O(4)$^{(1)}$-O(4)$^{(4)}$	4.02(1)	112.9(3)
	average	3.24	90.0
		M(3)	
	1 M(3)-O(3)	1.967(10)†	
	1 M(3)-O(9)	1.982(7)†	
	1 M(3)-O(11)	1.994(10)†	
	1 M(3)-O(10)	2.022(11)†	
	2 M(3)-O(12)$^{(1)}$	2.128(11)‡	
$z = ¼$	average	2.037	
	2 O(10)-O(12)$^{(1)}$	2.63(1)* **	78.6(5)
	2 O(11)-O(12)$^{(1)}$	2.68(1)*§	81.0(2)
	1 O(9)-O(11)	2.69(1)*§	85.1(3)
	1 O(3)-O(9)	2.78(1)	89.5(3)
	1 O(3)-O(10)	2.86(1)	91.5(3)
	1 O(10)-O(11)	2.93(1)	93.9(3)
	2 O(3)-O(12)$^{(1)}$	3.14(1)	100.2(2)
	2 O(9)-O(12)$^{(1)}$	3.18(1)	101.2(3)
	average	2.88	90.2
		Si(1)	
	3 Si(1)-O(8)	1.62(1)	
	1 Si(1)-O(1)	1.68(2)	
	average	1.63	
	3 O(8)-O(8)$^{(1)}$	2.64(1)	108.7(4)
	3 O(1)-O(8)	2.71(2)	110.3(3)
	average	2.67	109.5
		C(5)	
	1 C(5)-O(15)	2.222(15)	
	1 C(5)-O(9)	2.269(8)	
	2 C(5)-O(17)	2.281(6)	
	2 C(5)-O(13)	2.304(8)	
	1 C(5)-O(14)	2.443(12)	
	1 C(5)-O(11)	2.448(8)	
$z = ½$	average	2.319	
	2 O(13)-O(14)	2.55(1)* **	65.0(2)
	2 O(13)-O(17)	2.60(1)* **	69.0(3)
	2 O(11)-O(17)	2.61(1)* **	66.9(3)
	1 O(14)-O(15)	2.66(2)*§	69.3(6)
	1 O(9)-O(11)	2.69(1)*§	69.4(3)
	2 O(15)-O(17)	2.81(2)*§	77.1(3)
	2 O(9)-O(13)	2.86(1)*§	77.3(2)
	average	2.68	70.8
		M(2)	
	1 M(2)-O(2)	2.16(1)	
	1 M(2)-O(6)$^{(2)}$	2.21(1)	
	1 M(2)-O(4)	2.25(1)	
	1 M(2)-O(7)	2.25(1)	
	1 M(2)-O(7)$^{(2)}$	2.25(1)	
	1 M(2)-O(3)$^{(2)}$	2.27(1)	
	average	2.23	
	1 O(4)-O(7)	2.65(1)* **	72.1(4)
	1 O(3)$^{(2)}$-O(7)$^{(2)}$	2.71(1)* **	73.8(3)
	1 O(3)$^{(2)}$-O(6)$^{(2)}$	2.88(1)* **	79.8(3)
	1 O(2)-O(7)	2.94(1)* **	83.5(3)
	1 O(2)-O(7)$^{(2)}$	2.94(1)* **	83.5(4)
	1 O(4)-O(6)$^{(2)}$	3.06(1)* **	86.4(5)
	1 O(2)-O(4)	3.23(1)	94.1(4)
	1 O(6)$^{(2)}$-O(7)$^{(2)}$	3.32(1)	96.0(4)
	1 O(2)-O(3)$^{(2)}$	3.34(1)	97.7(2)
	1 O(6)$^{(2)}$-O(7)	3.40(1)	99.0(5)
	1 O(3)$^{(2)}$-O(4)	3.62(1)	106.2(3)
	1 O(7)-O(7)$^{(2)}$	3.64(1)	107.9(4)
	average	3.14	90.0
		M(4)	
	1 M(4)-O(10)$^{(2)}$	1.910(9)†	
	1 M(4)-O(4)	1.953(7)†	
	1 M(4)-O(13)	1.990(7)†	
	1 M(4)-O(9)	2.008(4)†	
	1 M(4)-O(8)	2.097(5)‡	
	1 M(4)-O(12)	2.224(5)‡	
	average	2.030	
	1 O(8)-O(9)	2.63(1)* **	79.5(2)
	1 O(10)$^{(2)}$-O(12)	2.63(1)* **	78.6(3)
	1 O(4)-O(10)$^{(2)}$	2.63(1)	85.7(4)
	1 O(12)-O(13)	2.74(1)*§	80.8(2)
	1 O(10)$^{(2)}$-O(13)	2.77(1)	90.7(3)
	1 O(8)-O(13)	2.79(1)	86.1(3)
	1 O(9)-O(13)	2.86(1)*§	91.2(3)
	1 O(4)-O(9)	2.86(1)	92.5(3)
	1 O(4)-O(8)	3.07(1)	98.6(3)
	1 O(8)-O(10)$^{(2)}$	3.07(1)	100.0(2)
	1 O(4)-O(12)	3.07(1)	94.4(2)
	1 O(9)-O(12)	3.18(1)	102.3(2)
	average	2.86	90.0
		Si(2)	
	3 Si(2)-O(12)	1.61(1)	
	1 Si(2)-O(2)	1.67(1)	
	average	1.62	
	3 O(12)-O(12)$^{(1)}$	2.61(1)	108.6(5)
	3 O(2)-O(12)	2.69(1)	110.3(3)
	average	2.65	109.5
		M(7)	
	1 M(7)-O(11)$^{(2)}$	1.869(4)†	
	1 M(7)-O(17)$^{(2)}$	1.870(11)†	
	1 M(7)-O(13)	1.904(11)†	
	1 M(7)-O(17)	1.935(10)†	
	1 M(7)-O(12)	2.307(6)‡	
	1 M(7)-O(18)	2.371(28)‡	
	average	2.043	
	1 O(13)-O(17)	2.60(1)* **	87.0(5)
	1 O(11)$^{(2)}$-O(17)$^{(2)}$	2.61(1)* **	86.6(3)
	1 O(11)$^{(2)}$-O(12)	2.68(1)*§	79.0(4)
	1 O(17)-O(18)	2.68(7)*§	81.8(25)
	1 O(11)$^{(2)}$-O(13)	2.72(1)	92.4(4)
	1 O(12)-O(13)	2.74(1)*§	80.5(4)
	1 O(17)-O(17)$^{(2)}$	2.78(1)	93.9(5)
	1 O(17)$^{(2)}$-O(18)	2.84(8)*§	77.3(13)

TABLE 4—*Continued*

		M(6)		1 O(13)-O(18)	3.20(3)	96.4(25)
	2 M(6)-O(14)$^{(1)}$	1.892(6)†		1 O(11)$^{(2)}$-O(18)	3.28(4)	100.8(13)
	2 M(6)-O(13)$^{(1)}$	1.900(8)†		1 O(12)-O(17)	3.28(1)	101.3(4)
	1 M(6)-O(16)	2.311(26)‡		1 O(12)-O(17)$^{(2)}$	3.29(1)	102.9(4)
	average	1.979		average	2.89	90.0
	2 O(13)$^{(1)}$-O(14)$^{(1)}$	2.55(1)* **	84.6(4)			
	2 O(14)$^{(1)}$-O(16)	2.63(3)*§	76.7(9)			
	1 O(14)$^{(1)}$-O(14)$^{(4)}$	2.78(1)	94.6(5)			
	1 O(13)$^{(1)}$-O(13)$^{(4)}$	2.83(1)	96.2(3)			
	2 O(13)$^{(1)}$-O(16)	3.34(3)	104.5(9)			
	average	2.83	90.3			
		M(8)			**M(9)**	
	1 M(8)-O(20)	1.988(8)†		1 M(9)-O(19)	1.936(3)†	
	1 M(8)-O(5)	1.900(11)†		1 M(9)-O(7)	1.951(7)†	
	1 M(8)-O(15)	1.946(22)†		1 M(9)-O(15)	1.997(12)†	
	1 M(8)-O(14)	1.936(10)†		1 M(9)-O(17)	2.006(8)†	
	1 M(8)-O(16)$^{(3)}$	2.211(22)‡		1 M(9)-O(18)	2.153(94)‡	
	1 M(8)-O(16)$^{(2)}$	2.211(22)‡		1 M(9)-O(18)$^{(1)}$	2.390(103)‡	
$z = \frac{3}{4}$	average	2.032		average	2.072	
	1 O(16)$^{(2)}$-O(20)	2.51(3)* **	73.0(9)	1 O(18)$^{(1)}$-O(19)	2.58(5)* **	72.3(12)
	1 O(16)$^{(3)}$-O(20)	2.51(3)* **	73.0(9)	1 O(18)-O(19)	2.58(5)* **	78.0(10)
	1 O(5)-O(20)	2.63(2)	85.1(10)	1 O(7)-O(19)	2.62(1)	84.7(5)
	1 O(14)-O(16)$^{(3)}$	2.63(3)*§	78.4(7)	1 O(17)-O(18)	2.68(7)*§	79.9(7)
	1 O(14)-O(15)	2.66(2)*§	86.4(6)	1 O(15)-O(17)	2.81(2)*§	89.1(5)
	1 O(14)-O(16)$^{(2)}$	2.63(3)*§	78.4(7)	1 O(17)-O(18)$^{(1)}$	2.84(8)*§	80.1(6)
	1 O(14)-O(20)	2.87(3)	94.0(10)	1 O(17)-O(19)	2.85(2)	92.8(5)
	1 O(5)-O(15)	2.82(2)	94.4(6)	1 O(7)-O(15)	2.87(1)	93.4(5)
	1 O(5)-O(16)$^{(3)}$	3.19(3)	101.4(7)	1 O(7)-O(18)	3.15(7)	98.7(6)
	1 O(15)-O(16)$^{(2)}$	3.35(3)	107.1(9)	1 O(15)-O(18)$^{(1)}$	3.17(8)	99.7(14)
	1 O(15)-O(16)$^{(3)}$	3.35(3)	107.1(9)	1 O(15)-O(18)	3.17(9)	110.7(14)
	1 O(5)-O(16)$^{(2)}$	3.19(3)	101.4(7)	1 O(7)-O(18)$^{(1)}$	3.30(8)	100.0(7)
	average	2.86	90.0	average	2.88	90.0
		Si(3)				
	2 Si(3)-O(18)	1.54(5)				
	1 Si(3)-O(16)$^{(2)}$	1.56(3)				
	1 Si(3)-O(6)	1.61(1)				
	average	1.56				
	2 O(16)$^{(2)}$-O(18)	2.37(10)	99.7(26)			
	1 O(18)-O(18)$^{(3)}$	2.59(8)	114.2(28)			
	1 O(6)-O(16)$^{(2)}$	2.60(3)	110.0(11)			
	2 O(6)-O(18)	2.66(3)	115.3(11)			
	average	2.54	109.0			

Note: Under each atom heading are listed bond distances [in increasing order of magnitude except M(8) to be compared with M(9)] and angles. Estimated standard errors refer to the last digit. Equivalent points refer to Table 3 and appear as superscripts in parentheses: (1) $-y, x-y, z$; (2) $y-x, -x, z$; (3) y, x, z; (4) $-x, y-x, z$; (5) $x-y, -y, z$.

* Shared edges between polyhedra.

** Shared edge at same level.

† Equatorial bond.

‡ Apical bond.

§ Shared edge at adjacent level.

Rather detailed descriptions with many sketches were given by Fanfani et al. (1975) for schairerite and by Moore and Araki (1977) for mitridatite. Schairerite has 56 atoms in the asymmetric unit, and mitridatite has 75. All three structures belong to polar symmetry groups. The unit formulas for the nonameric sheets can be written

långbanite	$Mn_9^{3+}O_6(SiO_4)(SiO_4)_2O_{18}$	$P31m$
schairerite	$Na_9^{1+}F_6(SO_4)(SO_4)_2O_{18}$	$P31m$
mitridatite	$Fe_9^{3+}O_6(PO_4)(PO_4)_2O_{18}$	$Aa.$

These sheets are normal to **c***, **c***, and **a***, respectively.

We propose to compare these sheets through direct assessment of their differences (Δ, Å) in atom positons by fixing one site in each structure, namely the corner-linking tetrahedron in the center of the nonamer. These correspond to Si(1), S(3), and P(7) in the three structures, respectively. As the sheets themselves belong to polar groups and as all 48 atoms in the mitridatite sheet are unique, the positions of the central tetrahedra in the three structures were set to (0.250, 0.000, 0.000) after the following cell transformations. The transformed cell translations are primed.

Mitridatite is monoclinic clinohedral (polar) with space group Aa, $a = 17.53$, $b = 19.35$, $c = 11.25$ Å, $\beta = 95.84°$, $a \sin \beta = 17.46$ Å and the cell contains $4\{Ca_6(H_2O)_6[Fe_9^{3+}O_6(PO_4)(PO_4)_2(PO_4)_6]\cdot 3H_2O\}$. Six sheets occur along [100]: ·Ca-Fe-Ca-Ca-Fe-Ca·. Note that $b/\sqrt{3} = 11.17 \sim c = 11.25$ Å. This sheet is markedly pseudotrigonal, with average $c' = 11.21$ Å. As långbanite has four sheets, $a' = \frac{1}{6} \times a \sin \beta = 11.64$ Å. An orthohexagonal cell is defined, that is, $b' = \sqrt{3}\, c' = 19.42$ Å. Schairerite, trigonal polar with space group $P31m$, $a = 12.20$, $c = 19.26$ Å, and cell

TABLE 5. Comparison of differences (Δ) for schairerite and mitridatite with respect to långbanite

L	S	Δ (Å)	M	Δ (Å)	L	S	Δ (Å)	M	Δ (Å)
M(3)	Na(1)	0.18	Fe(1)	0.44	O(3)	O(6b)	0.75	O(2)	0.57
M(3)	Na(1)	0.18	Fe(2)	0.39	O(4)	O(6c)	0.71	O(3)	0.49
M(3)	Na(1)	0.18	Fe(3)	0.41	O(4)	O(6c)	0.71	O(4)	0.53
M(4)	Na(1′)	0.18	Fe(4)	0.31	O(3)	O(6b)	0.75	O(8)	0.52
M(4)	Na(1′)	0.18	Fe(5)	0.36	O(4)	O(6c)	0.71	O(6)	0.51
M(4)	Na(1′)	0.18	Fe(6)	0.41	O(4)	O(6c)	0.71	O(7)	0.60
M(4)	Na(1′)	0.18	Fe(7)	0.44	O(3)	O(6b)	0.75	O(10)	0.47
M(4)	Na(1′)	0.18	Fe(8)	0.41	O(4)	O(6c)	0.71	O(11)	0.42
M(4)	Na(1′)	0.18	Fe(9)	0.27	O(4)	O(6c)	0.71	O(12)	0.47
Si(1)	S(3)	0.00	P(7)	0.00	O(11)	O(4b)	0.42	O(16)	0.40
O(1)	O(3a)	0.22	O(25)	0.50	O(13)	O(4c)	0.45	O(14)	0.44
O(8)	O(3b)	0.23	O(27)	0.21	O(13)	O(4c)	0.45	O(15)	0.27
O(8)	O(3b)	0.23	O(28)	0.21	O(11)	O(4b)	0.42	O(18)	0.52
O(8)	O(3b)	0.23	O(26)	0.23	O(13)	O(4c)	0.45	O(19)	0.48
Si(2)	S(3′)	0.36(0.98)	P(9)	1.33(0.98)	O(13)	O(4c)	0.45	O(20)	0.33
O(2)	O(3a′)	3.53(0.90)	O(33)	4.41(0.90)	O(11)	O(4b)	0.42	O(22)	0.58
O(12)	O(3b′)	0.71	O(34)	0.33	O(13)	O(4c)	0.45	O(23)	0.60
O(12)	O(3b′)	0.71	O(35)	0.25	O(13)	O(4c)	0.45	O(24)	0.50
O(12)	O(3b′)	0.71	O(36)	0.22	O(9)	F(3)	0.51	O(38)	0.49
Si(2)	S(3′)	0.36(0.97)	P(8)	1.33(0.97)	O(9)	F(3)	0.51	O(39)	0.55
O(2)	O(3a′)	3.53(0.91)	O(29)	4.41(0.91)	O(9)	F(3)	0.51	O(42)	0.55
O(12)	O(3b′)	0.71	O(30)	0.24	O(10)	F(1)	0.78	O(37)	0.18
O(12)	O(3b′)	0.71	O(31)	0.36	O(10)	F(1)	0.78	O(40)	0.29
O(12)	O(3b′)	0.71	O(32)	0.15	O(10)	F(1)	0.78	O(41)	0.27

Note: Differences, Δ (Å), for schairerite (S) and mitridatite (M) with respect to långbanite (L) cell are given. See text for references to atom coordinates. Values for inversions of certain tetrahedra are given parenthetically. The sheets compared correspond to $z = ¼$ in the real långbanite cell.

contents $3Na_{21}S_7O_{28}F_6Cl$, has seven sheets along [001]. Therefore, $a' = \frac{4}{7}c = 11.00$, $b' = \sqrt{3}a = 21.13$, and $c' = a = 12.20$ Å. The orthohexagonal cell of långbanite is $a' = c = 11.10$, $b' = a\sqrt{3} = 20.02$, $c' = a = 11.56$ Å.

The cells to be compared in orthohexagonal setting are

	a'	b'	c'	$a':b':c'$
långbanite	11.10	20.02	11.56	0.554:1:0.577
schairerite	11.00	21.13	12.20	0.521:1:0.577
mitridatite	11.64	19.42	11.21	0.599:1:0.577.

Obviously, differences among these cells arise from quite different compositions among the compounds, from the collapsing of different kinds of sheets, and from differences in charge.

All pertinent atom coordinates were transformed accordingly. The value of Δ (Å) was calculated with respect to the transformed långbanite cell ($a' \times b' \times c'$) for all cations and anions in the sheets. Table 5 lists these differences for 48 atom positions. The two Si(2) tetrahedra, each of which links to three nonamers, point in the same direction, but in the opposite direction for S(3′) of schai-

TABLE 5A. Differences of schairerite and långbanite atom coordinates from those of invariant lanthanum

	Schairerite													
	Atom	S	R		I		Δ (Å)		Atom	S	R		I		Δ (Å)
$z = ⅓$	S(7)	A	3	⅔	0	⅓	0.11	$z = ⅚$	S(4)	C	3	⅔	⅔	⅚	0.16
	Na(5)	A	3	⅙	⅙	⅓	0.20		Na(4)	C	3	⅙	0	⅚	0.20
	Na(5′)	A	6	⅜	⅔	⅓	0.40		Na(4′)	C	6	⅜	⅙	⅚	0.17
$z = ⅔$	S(1)	B	1	0	0	⅔	0.05	$z = ⅙$	S(2)	B	1	0	0	⅙	0.44
	S(1′)	B	2	⅓	⅔	⅔	0.44		S(2′)	B	2	⅓	⅔	⅙	0.12
	Na(7)	B	3	⅜	⅜	⅔	0.25		Na(6)	B	3	⅜	⅜	⅙	0.21
	Na(7′)	B	6	⅔	⅙	⅔	0.24		Na(6′)	B	6	⅔	⅙	⅙	0.23
$z = ⅜$	S(6)	A	3	⅔	0	⅜	0.12	$z = ⅞$	S(5)	C	3	⅔	⅔	⅞	0.10
	Na(2)	A	3	⅙	⅙	⅜	0.26		Na(3)	C	3	⅙	0	⅞	0.39
	Na(2′)	A	6	⅜	⅔	⅜	0.34		Na(3′)	C	6	⅜	⅙	⅞	0.25
$z = ⅓$	S(3)	B	1	0	0	⅓	0.15							Average	0.22 Å
	S(3′)	B	2	⅓	⅔	⅓	0.23							Range	0.05–0.44 Å
	Na(1)	B	3	⅜	⅜	⅓	0.19								
	Na(1′)	B	6	⅔	⅙	⅓	0.10								

Note: Atom coordinates from this study for långbanite and from Fanfani et al. (1975) for schairerite. The z coordinates for polar schairerite were increased by 0.056. Cations are arrayed according to fractional heights in z. The sequence of columns is atom site, stacking sequence (S), equipoint rank (R), invariant point for lanthanum (I), difference Δ (Å) based on långbanite and schairerite cells, respectively. Some layers in La were shifted to accommodate schairerite.

rerite and P(8) and P(9) of mitridatite. Therefore, approximate calculations were included in parentheses, as if these tetrahedra were reversed. Four sets of atoms fall into this category. Of the remaining 44 atoms, ten cations have average $\Delta = 0.16$ Å for schairerite and 0.34 Å for mitridatite, and 34 anions have average $\Delta = 0.57$ Å for schairerite and 0.40 Å for mitridatite. The grand average is 0.48 Å (range 0.00–0.78 Å) for schairerite and 0.39 Å (range 0.00–0.60 Å) for mitridatite.

Comparison of La atoms to långbanite and schairerite cations

The långbanite structure is based on a simple principle: the double hexagonal close-packing (·ch·) of cations along the *c*-axis. It is based on the La structure type which is assumed by 33 phases, including intermetallic compounds and elements such as the lanthanides Ce, Gd, La, Nd, Pr, Sm and the actinides Am, Bk, Cf, Cm, as tabulated by Villars and Calvert (1985). La has $P6_3/mmc$, $Z = 4$, $a = 3.770$, $c = 12.159$ Å; 2La(1) in (2a) $\bar{3}m$ (000), 2La(2) in (2c) $\bar{6}m2$ (⅓, ⅔, ¼). Transforming the *a*-axis to $a' = 2\sqrt{3}a = 13.06$ Å, an expanded cell with $(2\sqrt{3})^2(4) = 48$ La atoms occurs. The axial ratio is $c/a' = 0.931$. This corresponds to $c/a = 11.10/11.56 = 0.960$ for långbanite. Table 5a lists the invariant points of the transformed La cell and the difference (Δ) between analogous atomic positions of La and långbanite calculated with respect to the långbanite cell. The remarkable feature is that the 13 unique cation positions in långbanite are those of the invariant La atom positions, with average $\Delta = 0.17$ Å, and a range of 0.04–0.33 Å. Except for the brucite-like layer at $z = 0$, the anions in långbanite offer no suggestion of dense-packing principles.

This same treatment was applied to the schairerite structure as determined in the elegant study of Fanfani et al. (1975) and calculated as the difference between the positions of the ·chhchhc· invariant model and those of the 24 independent cations. The differences, Δ, are based on the schairerite cell and also appear in Table 5a. Again, an array of close-packed cations appears, with average $\Delta = 0.22$ Å and a range of 0.05–0.44 Å. This relationship between långbanite and schairerite is all the more remarkable when it is realized that the two compounds are chemically unrelated and their bonding is distinct; in addition, their parageneses—one occurs in an evaporite brine, the other in a well-developed skarn—are wholly unrelated. Again, there is no evidence that the anions are based on principles of closest packing. The $^2_\infty[M^{3+}_9T_3\phi_{36}]$ sheet of octahedral nonamers at $z = ¼$ in långbanite also occurs as the principal sheet in mitridatite (yet a different paragenesis) and as one of the seven unique layers in schairerite. The important phase, Ca_3OSiO_4 or alite, has an average structure based on nine layers that resemble the remaining six layers in schairerite and the layer at $z = ¾$ in långbanite. The difference calculations were not performed on this sheet because the Jeffery (1952) model for alite is only approximate. The alite cation packing sequence is 3·chh· per cell translation.

TABLE 5A—*Continued*

	Långbanite						
	Atom	S	R		I		Δ (Å)
$z = ¾$	M(1)	A	3	⅚	0	¾	0.06
	M(2)	A	6	⅜	⅔	¾	0.15
	Sb	A	3	⅔	0	¾	0.16
$z = ¼$	M(3)	B	3	⅜	0	¼	0.32
	M(4)	B	6	⅔	⅙	¼	0.16
	Si(1)	B	1	0	0	¼	0.23
	Si(2)	B	2	⅙	⅔	¼	0.20
$z = ½$	C(5)	A	3	⅔	0	⅔	0.12
	M(6)	A	3	⅚	0	⅔	0.04
	M(7)	A	6	⅜	⅔	⅔	0.18
$z = ¾$	M(8)	C	3	⅙	0	¾	0.20
	M(9)	C	6	⅜	⅙	¾	0.33
	Si(3)	C	3	⅙	0	¾	0.04
						Average	0.17 Å
						Range	0.04–0.33 Å

Cation close-packing schemes

A possible chemical crystallographic kinship of långbanite to braunite, tetragonal $Mn^{2+}_2Mn^{3+}_{12}Si^{4+}_2O_{24}$, was suggested by Strunz (1944). He found that the cubic cell analogous to bixbyite, upon suitable hexagonal cell transformation (b), mimicked the långbanite (l) cell. We used the value $a = 9.4146$ Å, space group $Ia\bar{3}$, and cell contents $16\alpha\text{-}(Mn_{0.98}Fe_{0.02})^{3+}_2O_3$ of bixbyite as reported by Geller (1971): $a(b) = (\sqrt{2}\sqrt{3}/2)a = 11.53$, $c(b) = (2\sqrt{3}/3)a = 10.87$ Å, $c(b)/a(b) = 2\sqrt{2}/3 = 0.943$. Our långbanite cell yields $c(l)/a(l) = 0.960$. Relative to långbanite, the transformed bixbyite cell parameter differences are $\Delta a = -0.03$, $\Delta c = -0.23$ Å.

Despite these similarities, the structures are only remotely related. In the full bixbyite hexagonal cell, $a(b) = \sqrt{2}a = 13.31$, $c(b) = \sqrt{3}a = 16.31$ Å and there are six cubic closest-packed cation layers; ·cc·, with intersheet separation of $16.31/6 = 2.72$ Å. In långbanite, the *c*-axis translation includes four closest-packed cation layers in double hexagonal close packing, ·ch·, with an interlayer separation of $11.10/4 = 2.77$ Å. It was discovered that filled cation layers at $z = ⅓, ⅔$ in armangite, with space group $P\bar{3}$, cell contents $1\square_3Mn^{2+}_{26}As^{3+}_{18}C^{4+}O_{54}\psi_{18}(H_4O_3)$, and $a = 13.49$, $c = 8.86$ Å (see Moore and Araki, 1979 for a description of this curious anion-deficient fluorite derivative structure with cation ·c· layers, in their Fig. 2b) bear uncanny resemblance to the bixbyite layers parallel to (111). Even the polyhedral distortions are similar, although armangite is a Mn^{2+} compound, whereas bixbyite is a Mn^{3+} compound. The formidable formula for armangite includes three ordered cation vacancies (□), 18 space-occupying lone pairs ψ associated with As^{3+}, and the disordered extraneous atoms in parentheses. Armangite, like långbanite, bixbyite, and braunite, is a Långban mineral.

In all structures here discussed, the packing principle is

TABLE 6. Långbanite shared polyhedral edges

	A		B			
Layer	A_1	A_2	B_1	B_2	C	D
$z = 0$	3 M(1)	12			18	36
	6 M(2)	12			36	72
	3 Sb	12			18	36
			72	0		Sum 144
$z = ¼$	3 M(3)	12			15	36
	6 M(4)	12			24	72
	1 Si(1)	6			0	6
	2 Si(2)	6			0	12
			9	30		Sum 126
$z = ½$	3 C(5)	12			36	36
	3 M(6)	8			12	24
	6 M(7)	12			36	72
			18	66		Sum 132
$z = ¾$	3 M(8)	12			15	36
	6 M(9)	12			30	72
	3 Si(3)	6			0	18
			9	36		Sum 126
			Sum 108	132	240	Total 528

Note: Each successive cation layer is listed according to fractional coordinates z; A = polyhedral edges, A_1 = equipoint and atom designation, A_2 = number of edges per polyhedron; B = edges shared in cell, B_1 = in-plane, B_2 = between-plane; C = edges shared in cell; D = total edges in cell. Further note that $B_1 + B_2 = C$ and $C/D \times 100 = 45.5\%$, the percentage of edges shared.

based on the close packing of cations. In many arrangements, the cations are not by themselves based on any such packing principles, at least according to prevailing dogma. Because descriptions of inorganic crystal structures are traditionally based on anion close packing, such structures in the past were obscured through discussion of anions only. Volume packing efficiency, V_E, in hortative. Here all atoms of one kind, say anions (ϕ) or cations (X), in a unit cell are divided into the unit-cell volume; V_E can be directly related to an ion's radius. In the close packing of spheres, the proportion of space occupied by spheres is $\pi/\sqrt{18}$. What about the volume packing efficiency? This can be easily expressed by noting that the sphere's volume, $4/3\pi r^3$, must be multiplied by the reciprocal of the space occupied by spheres in close packing, e.g., $V_E = (4/3\pi r^3)(\sqrt{18}/\pi) = 4\sqrt{2}r^3$. Thus, for Pauling radii $r^{[6]}O^{2-} = 1.40$ Å, $V_E/O^{2-} = 15.52$ Å^3; and for $r^{[6]}S^{2-} = 1.84$ Å, $V_E/S^{2-} = 35.23$ Å^3. In oxysalts, the calculation divides the total number of close-packed ions in the unit cell into the unit cell volume. What about radius ratios that are considerably greater than the lower limit? For octahedral coordination of anions about cations, $r_+/r_- = 0.414$. For $^{[6]}Ca^{2+}{}^{[6]}O^{2-}$, $r_+/r_- = 1.00/1.40 = 0.714$. Thus in 4CaO, $Fm3m$, $a = 4.81$ Å, $V_E/O^{2-} = 27.8$ Å^3, corresponding to $rO^{2-} = 1.70$ Å. Clearly, radius ratio is only a very rough predictor of coordination number. And a paradox remains: ionic size has very little meaning, other than some effective means of tabulating values for future additivity relationships (such as bond distances). We shall bypass this paradox by concentrating only on packing efficiency.

Polyhedral distances and distortions

Emphasis so far has been placed on the four unique sheets that comprise långbanite's structure. Yet the sheets are not insular entities but are linked to adjacent sheets through sharing of corners or edges or both. No shared faces occur in the långbanite structure. The shared corners and edges were obtained in the following way: The individual sheets (Figs. 1a to 1d) immediately gave the in-plane linkages of shared corners and edges. The between-plane shared edges were counted by constructing a matrix and consulting Table 4 of bond distances and angles. In this manner, edges within the plane of a sheet and edges between the sheets could be counted. All polyhedra in the unit cell were isolated to derive the count of total polyhedral edges in that cell. An inventory, layer by layer, is given in Table 6.

Of a total of 528 available polyhedral edges for cations coordinated by anions in the långbanite cell, 240 (45.5%) are shared between polyhedra. The remaining 54.5% of available edges, which includes all 36 tetrahedral edges of $[SiO_4]$, are not shared. For the brucite-like sheet at $z = 0$, no edges are shared between the sheets. The greatest number of shared edges is associated with the fundamental hexagonal alunite-jarosite $^2_\infty M\phi_4$ sheet at $z = ½$, where the largest number of between-plane shared edges (66) occurs.

The shared edges are noted accordingly in Table 4 of polyhedral distances and angles. All distances for individual polyhedra are arrayed according to increasing distance values unless indicated otherwise. The O-M-O′ angles are listed according to the corresponding O-O′ edges. From cation-cation repulsion effects across shared edges according to Pauling's (1960) third rule, the cations will move away from each other. This will force a polyhedral distortion with shortening of the polyhedral shared edge(s) relative to the unshared edges and diminution of polyhedral angle(s) associated with these shared edges. This trend can be immediately recognized in Table 4. Therefore, arranging polyhedral distances and angles according to increasing values makes good sense because the shared edges and associated angles should occur toward the tops of individual polyhedral entries.

Finally, the apical elongation and equatorial compression expected for the Jahn-Teller ion $4d^4$ Mn^{3+} O octahedron deserves comment. The $Mn^{3+}O_6$ octahedra occur at $z = ¼, ½, ¾$. Without exception, the two in-plane Mn^{3+}-O elongate apical distances for each polyhedron occur at $z = ¼$ and ¾; two between-plane Mn^{3+}-O elongate apical distances for each polyhedron occur at $z = ½$ with respect to the central Mn^{3+} cation. In addition, all nine unique O-O′ polyhedral in-plane distances (= ** in Table 4) for Mn^{3+} are shorter than all the 15 unique O-O′ between-plane distances (= § in Table 4) for each Mn^{3+} polyhedron. These (** and §) and the apical (a) and equatorial (e) distances are so designated in Table 4. One polyhedron, $M(6)^{3+}O_5$, is a distorted square pyramid, with average M(6)-O = 1.896 Å for four equatorial distances and M(6)-O(16) = 2.311 Å for the sole apical distance. The

$M(3)^{3+}$-O and $M(4)^{3+}$-O distances do not display the pronounced elongate square bipyramidal character expected of $Mn^{3+}O_6$, and we speculate that Fe^{3+} reported in the probe analysis occurs extensively at these sites. The average M-O distances of $M(7)^{3+}$, $M(8)^{3+}$, and $M(9)^{3+}$ assumed to be nearly pure Mn^{3+} sites are Mn^{3+}-O = 1.936 for the equatorial average (12 individual distances in toto), 2.274 Å for the apical average (six individual distances in toto), and 2.049 Å for the polyhedral average.

The C(5) (C for cube) site has cubic coordination with longer distances. It presumably accommodates Mn^{2+} and minor Ca^{2+} and Y^{3+}. The average distance is C(5)-O = 2.319, close to the value 2.327 Å found for a similar site in braunite, $Mn^{2+}Mn_6^{3+}Si^{4+}O_{12}$, by Moore and Araki (1976). All 12 edges of $C(5)O_8$ are shared with other polyhedra. The most pronounced distortions occur for the $M(1)^{2+}O_6$ octahedron. Pronounced cation-cation repulsion effects occur for two opposing edges shared with highly charged $Sb^{5+}O_6$. Edge distances for $M(1)O_6$ range from short O(4)-O(5) = 2.67 Å shared with SbO_6, whereas O(5)-O(5) = 3.85 Å, and O(4)-O(4) = 4.02 Å are the longest edges. These distances span the opposing SbO_6 octahedra. The bond distances M(1)-O(5) = 2.34 and M(1)-O(4) = 2.41 Å are also unusually long distances for $^{[6]}Mn^{2+}$-O, again a consequence of cation-cation repulsion. Noteworthy is the angle O(4)-M(1)-O(5) = 68.3° associated with the O(4)-O(5) = 2.67 Å distance, for the edge shared between M(1) and the Sb^{5+} polyhedron.

Asymmetric units of långbanite and related structures: a comparison

All structures that we now compare are based on sequences of cation close packing as follows: cubic fluorite and bixbyite, ·c· and ·cc· along [111]; trigonal armangite, ·c· along [001]; trigonal långbanite, ·ch·, a four-layer repeat along [001]; trigonal schairerite, ·chhchhc·, a seven-layer sequence. We use the condensed nomenclature, with the sequences of cubic close-packed layers designated ·c· (≡ ABC) or the hexagonal closest-packed sequence designated ·h· (≡ ABA). In principle, layer sequences of different types are identical in volume-packing efficiency for equal spheres. To a first approximation, therefore, we shall compare these different arrangements in the mineral crystals.

The respective structures were referred to unit cells with hexagonal geometries. The asymmetric unit chosen for comparison is a wedge that includes one-sixth of the cell. Populations at its vertices (× fractional occupancy for stoichiometric balance) are (xy) = (0, 0) × ⅙, (½, 0) × ¼, (½, ½) × ¼, (⅔, ⅓) × ⅓. These add up to ⅙ + ¼ + ¼ + ⅓ = 1. An atom on a bounding line of the wedge is ×½. An atom inside the wedge is ×1. In addition, individual layers are given symbols in full closest-packing nomenclature A, B, or C. Heights along z are given fractional coordinates. The five structures whose cation loci are featured appear in Figures 2a–2e.

Figure 2a shows fluorite referred to a hexagonal cell. Fluorite has a = 5.46 Å, space group $Fm\bar{3}m$, Z = 4. The hexagonal parameter a(h) was doubled for stoichiometric reasons, so $a(h) = 2\sqrt{2}a = 15.44$, $c(h) = \sqrt{3}a = 9.46$ Å. There are $4(2)^2(\sqrt{2})^2(\sqrt{3})\sqrt{3}/2 = 48$ CaF_2 in the hexagonal cell or ⅙(48) = 8 CaF_2 in the wedge which contains 8 asymmetric units of structure. The ratio $c(h)/a(h) = \sqrt{3}/2\sqrt{2} = 0.6125$. All Ca atoms, which are fixed points, are drawn in Figure 2a as solid circles. Only some of the F positions are included. Note that CaF_2 cubes were drawn. Fluorite is based on ·c· packing of cations.

Figure 2b shows bixbyite structure relations referred to a hexagonal cell. Bixbyite has a = 9.415 Å, space group $Ia\bar{3}$, and cell contents $16Mn_2^{3+}O_3$. The parameter c(h) was halved for the I centering and for comparative purposes, but the full-cell z fractional coordinates appear in Figure 2b. Thus $a(h) = \sqrt{2}a = 13.30$ Å, $c(h) = \frac{1}{2}\sqrt{3}a = 8.15$ Å, and $c(h)/a(h) = 0.6125$. Ideal invariant close-packed positions appear as crosses and cation positions as solid circles in this figure. The hexagonal cell has $32(\sqrt{2})^2(\frac{1}{2}\sqrt{3})\sqrt{3}/2 = 48$ Mn^{3+} or ⅙(48) = 8 Mn^{3+} in the wedge which contains four asymmetric units. Note that doubling of the z-fractional coordinates leads to a close correspondence with invariant Ca positions in fluorite. Wells (1975) gives a related presentation of these anion deficient fluorite structures. Note that the shifts of Mn^{3+} cations from invariant close-packed positions are small. The cell with halved c(h) is based on ·c· packing of cations.

Figure 2c features the cation asymmetric unit of the complex armangite crystal structure. No transformations are required for this complex trigonal structure which has space group $P\bar{3}$, a = 13.491, c = 8.855 Å, and c/a = 0.6564. This astonishing structure has all unique cations, $C^{4+}_{1/6}Mn^{2+}_{2/6}\square_{3/6}Mn^{2+}_4As^{3+}_3$, or 8 cation positions including □ = ordered vacancy, in its asymmetric unit. Moore and Araki (1979) gave a mean value for Δ = 0.26 Å (range 0.00–0.63 Å) for nine unique cations, where Δ is the difference from perfect closest-packed invariant positions. Note that halved z coordinates in parentheses can be directly compared with those of the bixbyite unit having full c in Figure 2b.

The most remarkable feature is the relation between the positions of cations in bixbyite to those equivalent cation positions in armangite. This can be easily expressed by writing out the hexagonal cell contents (cation sum = 48): bixbyite $M(1)^{3+}$ $M(1)^{3+}_2$ $M(1)^{3+}_3$ $M(1)^{3+}_6$ $M(2)^{3+}_6$ $M(2)^{3+}_6$ $M(2)^{3+}_6$ $M(2)^{3+}_6$ $M(2)^{3+}_6$ $M(2)^{3+}_6$; armangite C^{4+} $M(1)^{2+}_2\square_3$ $M(2)^{2+}_6$ $M(3)^{2+}_6$ $M(4)^{2+}_6$ $M(5)^{2+}_6$ $As(1)^{3+}_6$ $As(2)^{3+}_6$ $As(3)^{3+}_6$. In bixbyite, 0/48 or 0% of the cations are missing from the close-packed frame. In armangite, 3/48 or 6% of the cations are missing. In bixbyite, 24/96 or 25% of the anions are missing. In the armangite structure, 42/96 or 44% of O anion positions are vacant. Occupied anion positions have a mean value of Δ = 0.46 Å (range 0.15–0.89 Å) as a measure of the difference from perfect closest packing. The mean cation charge for bixbyite is +3.00; for armangite, it is +2.29.

These relations, i.e., comparison of cation sites of different charges and a rather close approximation of posi-

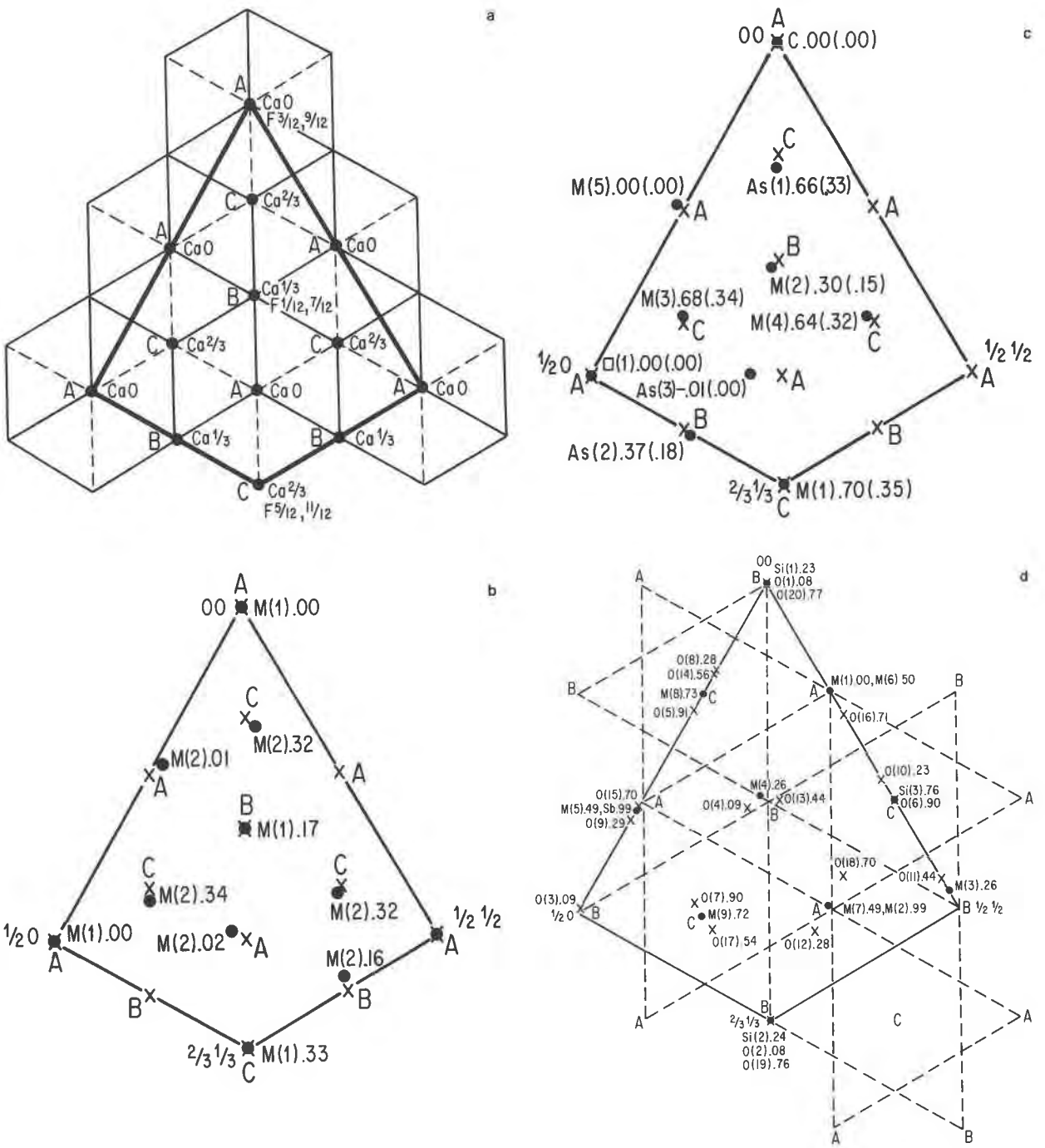

Fig. 2. The outline (0 0; ½ 0; ½ ½; and ⅔ ⅓) of related cells. Those of långbanite and schairerite are asymmetric units. Armangite is an asymmetric unit, and the metrically related compound cells of bixbyite and fluorite are also presented for purposes of comparison. (**a**) The compound cell of fluorite features 8Ca at $z = 0$, ⅓, and ⅔. Some F positions are included. The cubic closest-packed layers are designated at the nodes by A, B, and C. The [CaF_8] cubes along [111] are sketched in. (**b**) Compound cell of bixbyite cations. The centroids for perfect closest packing appear as crosses. The heights correspond to the full bixbyite cell and must be doubled to compare with fluorite. Note the tight fit of positions of bixbyite cations with those of fluorite. (**c**) All cations in the armangite asymmetric unit are shown. These can be compared directly with fluorite, or with bixbyite by halving the heights which are given in parentheses. Again, note the tight fit with positions of closest-packed centroids shown as crosses. (**d**) All cations and anions in the långbanite asymmetric unit. The A and B layers are dashed, C is in hexagonal centers. This arrangement and that of **e** are rotated $\pi/6$ radians with respect to **a–c**. Note the tight fit of cations and the scatter in anion positions with respect to nodal centers. The sequence for cations is ·ch·.

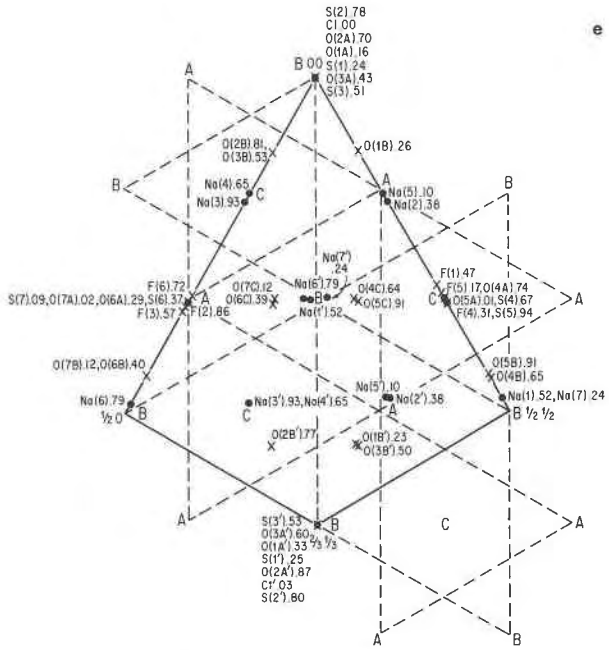

Fig. 2—*Continued.* (**e**) All cations and anions in the schairerite asymmetric unit. Instructions follow **d**. The unit contains 14 cations in a seven-layer repeat. (Note $14 \times 4/7 = 8$ as in långbanite.) Note the tight fit of cations and the scatter in anion positions with respect to the nodal centers. The sequence for cations is ·chhchhc·.

tions to those of close-packed invariant points and a wide difference among anion occupancies, speak strongly in favor of a cation-dominated structure model, even though the compositions and stoichiometries of bixbyite and armangite are markedly different.

Figure 2d (långbanite) and Figure 2e (schairerite) are for true asymmetric units, of the same space group, $P31m$. Inspection of these figures and requirements implicit in the space groups show that the asymmetric units are rotated by $\pi/6$ radians around the c-axis with respect to the structures in Figures 2a–2c. The långbanite structure has four layers of type ·ch· (≡ ·ABAC·), and its asymmetric unit contains eight cations. Note that $(2/\sqrt{3})a = 13.35$ Å for långbanite, compared with $\sqrt{2}a = 13.30$ Å for bixbyite. This is the key relationship found by Strunz (1944). In Figures 2d and 2e, the A layers as well as the B layers are connected by dashes. The C layers reside in the hexagonal windows which remain. Stoichiometry is also satisfied for schairerite. It has $Na_{63}S_{21}$ or $(63 + 21)/6 = 14$ cations in the asymmetric unit. As schairerite has a seven-repeat layer structure and as långbanite has a four-repeat unit, then $14(4/7) = 8$ cations occur for the same aliquot as in långbanite.

Relation to close-packing among cations in these structures was discussed in considerable detail (cf. Tables 5 and 5a). Figures 2d and 2e show cation centroids as solid circles and anion centroids as crosses. The contrast pattern is striking: whereas the cation positions are very similar to those of ideal closest-packed centroids, the anions show no such relation. We are forced to conclude that all such structures discussed in this study are based on principles of cation close packing.

A COMMENT

Of the large number of so-called close-packed structures, very few of the more complex examples have been proven to be such by any means. The result is a plethora of ill-defined structures. As a first approximation toward a more sensible set of relations, we have focused on (1) 3^6 connection within the plane, (2) stacking sequence normal to that plane, and (3) the parameter, Δ (Å), as a measure of the difference between the perfect closest-packed scheme and the real structure. A crucial decision may involve Dirichlet domain analysis (David and David, 1982; Moore, 1989).

Expression of close packing solely on the basis of the larger anions has been perpetuated through an abundance of early crude structure determinations. Many of these early determinations were first selected on the basis of cell parameters that suggested closest-packed anion geometries. Thus the structures of diamond, sphalerite, rocksalt, spinel, the olivines, and the humites were among the earliest minerals whose structures were solved. The first structure solution of bixbyite, α-Mn_2O_3, created a controversy (Glusker et al., 1987). The relative sizes of cations and anions (radius ratio) and their respective formal charges were major factors. To this day, anion dense packing is stressed, presumably because the radius of O^{2-} is larger than those of the cations concerned, e.g., O^{2-} ions pack closely and the cations fit in the interstices. The closest-packed frame is stressed in reports of structures, and only rarely is a mention bestowed upon the dispositions of the interstitial cations. The cations, too, have geometrically fixed positions in the close-packed model, but these are rarely compared with those of ideal close packing.

Size alone seems to have relegated cations as interstitial ions. Is it possible that cations could provide the close-packed frame? This occurs in the myriad of antistructures where cations and anions are switched when referred to a structure type, e.g., CaF_2 (fluorite)–OLi_2. Particularly inconclusive are the radius ratio relations $^{[8]}Ca^{2+}/^{[4]}F^- = 1.12/1.31 = 0.855$ and $^{[8]}O^{2-}/^{[4]}Li^+ = 1.42/0.59 = 2.407$. (All radii in this paper, unless otherwise stated, are from Shannon and Prewitt, 1969.) But if ionic radius has any meaning, what about charge per unit surface area? Here the classic model is taken literally: ions are charged spheres. Only 26% of the structures mentioned in Deer et al. (1966) are close packed, a particularly bad batting average.

It appears that, beyond radius ratio, there is another key relation: in a compound $X_r^{+n}\phi_s^{-q}$, there are interactions of the types (X-X'), (ϕ-ϕ') and (X-ϕ). The first two are designated repelling Coulomb forces; the last, we call attracting Coulomb forces. Conventional wisdom declares that the attracting forces must exceed the repelling forces. But this says nothing about the arrangements of ions. For example, what if (X-ϕ) are strongly attracting but (X-X')

Table 7. Långbanite bond valences and assorted bond sums

Cations	Anions O(1)	O(2)	O(3)	O(4)	O(5)	O(6)	O(7)
M(1)	3(2/6) 0.359(× 1)→ × 3↓			2/6 0.194(× 2)→ × 1↓	2(2/6) 0.229(× 2)→ × 2↓	2/6 0.359(× 1)→ × 1↓	
M(2)		3(2/6) 0.359(× 1)→ × 3↓	2(2/6) 0.271(× 1)→ × 2↓	2/6 0.285(× 1)→ × 1↓		2(2/6) 0.315(× 1)→ × 2↓	2(2/6) 0.315(× 1)→ × 2↓
M(3)			3/6 0.588(× 1)→ × 1↓				
M(4)				3/6 0.580(× 1)→ × 1↓			
M(7)							
M(8)					3/6 0.675(× 1)→ × 1↓		
M(9)							3/6 0.583(× 1)→ × 1↓
C(5)							
M(6)							
Sb			5/6 0.717(× 1)→ × 1↓	5/6 0.852(× 2)→ × 1↓	5/6 0.738(× 1)→ × 1↓		5/6 0.768(× 2)→ × 1↓
Si(1)	4/4 0.870(× 1)→ × 1↓						
Si(2)		4/4 0.895(× 1)→ × 1↓					
Si(3)						4/4 1.057(× 1)→ × 1↓	
				Anion sum (↓)			
P	2.00 (+2.6)	2.00 (+1.5)	2.00 (+9.9)	2.00 (+4.7)	2.00 (+7.0)	2.00 (−2.4)	2.00 (+1.0)
B	1.95	1.97	1.82	1.91	1.87	2.05	1.98
KM	2.00 (+2.6)	2.00 (+1.5)	2.08 (+14.3)	2.08 (+8.9)	2.08 (+11.2)	2.00 (−2.4)	2.08 (+5.1)

Note: Bond valences and multiplicities show horizontal arrows for cation-valence sums and vertical arrows for anion-valence sums. The valence sums calculated according to Pauling (1929) (P), Brown (1981) (B) and Kampf and Moore (1976) (KM) conclude the anion sums. The Brown (1981) sums are used as a reference, deviations from which are given in parentheses as percent. Pauling and Brown bond strengths (valences) are given as bond entries.

are strongly repelling? Is it possible that X atoms can arrange in space to maximize mutual separations yet conserve (X-ϕ) attraction? We postulate that repelling ions in a given confining space adopt the same configuration as attracting ions in that same confining space. The asserted configuration is based on close packing. This has certain implications. It suggests, on the one hand, anions ($\phi - \phi'$) can assume closest packing with cations at interstices to optimize (X-ϕ) attractions. Nothing can be said about the dispositions of these cations. On the other hand, there is a region beyond which cations adopt close packing, but nothing can be said about the anions other than that their configurations optimize (X-ϕ) attractions.

From this, three classes of crystal structures can be conceived which are concerned with close packing. In the first, anions define the close-packed frame with unspecified cation positions at interstices. In the second, cations define the close-packed frame with unspecified anion populations coordinating to them. These first two models stress the structure-antistructure, e.g., CaF_2-OLi_2 duality. The third possibility is that cations and anions are indistinguishable, as in the MX rocksalt-type structures. It is interesting to note that the vector sets for the first two are the same according to position but differ in density and that the loci of M and X in the third are indistinguishable both according to position and density. The structure-antistructure model, stressed by O'Keeffe and Hyde (1985), may well provide the impetus to explore Ewald's (1973) electrostatic energy of a crystal as a vector space.

It is concluded, with the abundance of both simple and complex structure types, that are based on the close packing of cations rather than of anions and with the extraor-

TABLE 7—*Continued*

	Anions						
	O(8)	O(9)	O(10)	O(11)	O(12)	O(13)	O(14)
M(1)							
M(2)							
M(3)		3/6 0.549(× 1)→ × 1↓	3/6 0.479(× 1)→ × 1↓	3/6 0.518(× 1)→ × 1↓	3/6 0.362(× 2)→ × 1↓		
M(4)	2(3/6) 0.393(× 1)→ × 2↓	2(3/6) 0.498(× 1)→ × 2↓	2(3/6) 0.655(× 1)→ × 2↓		3/6 0.284(× 1)→ × 1↓	3/6 0.523(× 1)→ × 1↓	
M(7)				2(3/6) 0.737(× 1)→ × 2↓	3/6 0.232(× 1)→ × 1↓	3/6 0.668(× 1)→ × 1↓	
M(8)							3/6 0.610(× 1)→ × 1↓
M(9)							
C(5)		2/6 0.272(× 1)→ × 1↓		2/6 0.178(× 1)→ × 1↓		2/6 0.250(× 2)→ × 1↓	2/6 0.180(× 1)→ × 1↓
M(6)						3/6 0.675(× 2)→ × 1↓	2(3/6) 0.689(× 2)→ × 2↓
Sb							
Si(1)	4/4 1.028(× 3)→ × 1↓						
Si(2)					4/4 1.057(× 3)→ × 1↓		
Si(3)							
				Anion sum (↓)			
P	2.00 (+10.5)	1.75 (−3.8)	1.50 (−16.2)	1.75 (−19.4)	2.50 (+28.9)	1.85 (−12.7)	1.95 (−10.1)
B	1.81	1.82	1.79	2.17	1.94	2.12	2.17
KM	1.67 (−7.7)	2.00 (+9.9)	1.75 (−2.2)	2.00 (−7.8)	2.00 (+3.1)	2.09 (−1.4)	2.16 (−0.5)

dinarily diverse mimicry of successive sheets of långbanite to those of such similar units that are both simple and complex, that our understanding of the origins of structure type per se is poor and a huge field of further investigation is open.

Bond valence and bond strength sums for långbanite

It is often asked if bond length–bond strength correlations have much meaning in contemporary crystallographic studies. After all, structures can now be refined to a high level of precision. The Pauling (1929) electrostatic valence rule applied to predominantly ionic crystals, at least historically, is easily the most famous for quick checks of the plausibility of structures. It served very well in the early period of inorganic structure analysis when relatively simple compounds involving spherical (closed shell) ions were studied, deviations from anion neutrality being less than $\pm 1/6$ electrostatic unit (esu). In more recent times, with the appearance of ever more complex structures, the rule of Pauling appears to have fallen out of favor. These rules seem to work for spherical ions but are not helpful for systems involving lone-pair cations and the somewhat related cations exhibiting Jahn-Teller distortion of the bonded anion polyhedra. The advantage of the Pauling rule is its simplicity: it is based on individual bond strength computed from cation charge divided by the coordination number (the anions bonded to that cation). Essentially, the rule involves integers and, as such, constitutes a kind of average or tendency. The deviation of bond strength sum about an anion tends to be related to deviation of bond length from the cation-anion polyhedral average. Arraying the cations in långbanite ac-

TABLE 7—*Continued*

	Anions						Cation sum (→)
	O(15)	O(16)	O(17)	O(18)	O(19)	O(20)	
M(1)							1.56
M(2)							1.86
M(3)							2.83
M(4)							2.93
M(7)			2(⅜) 0.610(× 1)→ × 1↓ 0.737(× 1)→ × 1↓	⅜ 0.200(× 1)→ × 1↓			3.18
M(8)	⅜ 0.592(× 1)→ × 1↓	2(⅜) 0.293(× 2)→ × 2↓				3(⅜) 0.597(× 1)→ × 3↓	3.06
							2.74
M(9)	2(⅜) 0.513(× 1)→ × 2↓		⅜ 0.501(× 1)→ × 1↓	2(⅜) 0.191(× 1)→ × 1↓ 0.340(× 1)→ × 1↓	3(⅜) 0.610(× 1)→ × 3↓		1.96
C(5)	⅜ 0.305(× 1)→ × 1↓						
M(6)		⅗ 0.230(× 1)→ × 1↓	⅜ 0.263(× 2)→ × 1↓				2.96
Sb							4.70
Si(1)							3.95
Si(2)							4.07
Si(3)		¼ 1.214(× 1)→ × 1↓		¼ 1.284(× 2)→ × 1↓			4.84
			Anion sum (↓)				
P	1.75 (−8.9)	2.60 (+28.1)	1.75 (−17.1)	2.50 (+23.8)	1.50 (−18.0)	1.50 (−16.2)	
B	1.92	2.03	2.11	2.02	1.83	1.79	
KM	2.00 (+4.2)	2.00 (−1.5)	2.00 (−5.5)	2.00 (−1.0)	1.75 (−4.4)	1.75 (−2.2)	

cording to formal charge and coordination number, six distinct categories emerge: $^{[8]}M^{2+}$-C(5); $^{[6]}M^{2+}$-M(1),M(2); $^{[6]}M^{3+}$-M(3),M(4),M(7),M(8),M(9); $^{[5]}M^{3+}$-M(6); $^{[4]}T^{4+}$-Si(1),Si(2),Si(3); and $^{[6]}Sb^{5+}$-Sb.

A variation of the Pauling electrostatic valence rule was suggested by Kampf and Moore (1976) to explain pronounced deviations from neutrality when the spherical model was applied to bermanite, $Mn^{2+}(H_2O)_4[Mn_2^{3+}(OH)_2(PO_4)_2]$. The most pronounced deviations involved Mn^{3+}-O bonds. The four equatorial bonds (short) were empirically assigned $s = 7/12$ esu, and the two apical bonds (long) were assigned $s = 4/12$ esu. The sum of all six square bipyramidal bonds gave $4(7/12) + 2(4/12) = 3.00$ esu, the ionic charge on Mn^{3+}. An empirical assignment has been made for the Mn^{3+} tetragonal pyramid as well. This is $s = 8/12$ esu for the equatorial bonds and $s = 4/12$ esu for the apical bond. The sum of five bonds is $4(8/12) + 1(4/12) = 3.00$ esu. These assignments are appealing, as the equatorial bond strengths for the square pyramid should lead to shorter distances than those for the square bipyramid, and the apical bonds should be about the same length. This is what is observed in Table 4.

The bond valence rule of Brown (1981) proceeds from fitted constants for a particular bond pair and the individual observed bond distance, which are put into an inverse power or logarithmic function from which bond valence is calculated. The sums of the bond valences to cation and anion approximate the charges on the respective ions. These calculated charges can be compared with the individual bond valences to estimate degrees of underbonding and overbonding to the ions.

The recipes for Pauling bond strength sum, the modified Pauling sum of the Mn^{3+} prolate ellipsoids as given above, and the Brown bond valences were calculated. We included the Brown bond valences in Table 7 and used the Brown bond valence sums as the reference to compare with the other calculations. The first sums are based on the bond strengths of Pauling (P), the second sums correspond to the Brown (B) bond valences, and the third sums correspond to the prolate sphere model of Kampf and Moore (KM). A difference, Δ (%), was taken between each of the 20 unique anions referred to the approximate Brown bond valence sum, and the remainder was expressed in parentheses as percent in Table 7.

The contrast is striking. The Pauling spherical model has average magnitude difference of 12.1% with range $|\Delta| = 1.0$–28.9%. For the Kampf and Moore (1976) prolate sphere model, the magnitude difference is 4.9% with a range $|\Delta| = 0.5$–14.3%. In the Brown (1981) model, distances that are longer than the corresponding Pauling bond average are often called underbonded, and those that are shorter are called overbonded.

This may explain the unusually short Si(3)-O(16) 1.56 and Si(3)-O(18) 1.54 Å with normal Si(3)-O(6) 1.61 Å in Table 4. The atoms O(16) and O(18) are associated with unusually long Mn^{3+}-O distances, that is, they are substantially underbonded; however, Si(3)-O(16) and Si(3)-O(18) give $s = 1.21$ and 1.28 esu, respectively. This is supported by the Kampf-Moore model, where all differences, Δp_0, are within 2.5% for all Si(3)-O bonds. In this and the Brown models, O(16) and O(18) are very nearly neutral, suggesting that octahedral $4d^5$ Fe^{3+} at the M(8) and M(9) sites may not be stable and that långbanite owes its stability to the $4d^4$ Mn^{3+} square bipyramidal cation. The O(10), O(19), and O(20) anions are extremely undersaturated ($\Delta = -0.50$ esu) for the Pauling model. Each of these anions is coordinated by three Mn^{3+} cations. The anions receive the short equatorial bonds and are more neutralized thereby, using the Brown and the Kampf-Moore models in Table 7.

Acknowledgments

Ian M. Steele (University of Chicago) performed his usual superb Cameca probe analysis on a portion of the långbanite used in structure study. John S. White, Jr. of the U.S. National Museum provided the B-18215 sample, and we thank him for some fine crystals. John M. Hughes (Miami University in Ohio) pored through this cumbrous manuscript and sagaciously offered many suggestions toward its improvement.

P.B.M. acknowledges support by the National Science Foundation (grant EAR-8707382), and P.K.S. thanks the Tennessee Earthquake Information Center for use of their VAX computer.

References cited

Brown, I.D. (1981) The bond valence method: An empirical approach to chemical structure and bonding. In M. O'Keeffe and A. Navrotsky, Eds., Structure and bonding in crystals, vol. 2, p. 1–30. Academic Press, New York.

David, E.E., and David, C.W. (1982) Voronoi polyhedra as a tool in studying solvation structure. Journal of Chemical Physics, 76, 4611–4614.

Deer, W.A., Howie, R.A., and Zussman, J. (1966) An introduction to the rock-forming minerals, 528 p. Wiley, New York.

Ewald, P.P. (1973) Diffraction data and electrostatic energy of a crystal. American Crystallographic Association Summer Meeting Program and Abstracts, Series 2, vol. 1, 122.

Fanfani, L., Nunzi, A., Zanazzi, P.F., and Zanzari, A.R. (1975) The crystal structure of schairerite and its relationship to sulphohalite. Mineralogical Magazine, 40, 131–139.

Flink, G. (1887) Über Långbanit, ein neues Mineral von Långbanshyttan in Wermland, Schweden. Zeitschrift für Kristallographie, 13, 1–8.

Geller, S. (1971) Structures of α-Mn_2O_3, $(Mn_{0.983}Fe_{0.017})_2O_3$ and $(Mn_{0.37}Fe_{0.63})_2O_3$ and relation to magnetic ordering. Acta Crystallographica, B27, 821–828.

Glusker, J.P., Patterson, B.K., and Rossi, M. (1987) Patterson and Pattersons: Fifty years of the Patterson function, p. 34–44. International Union of Crystallography, Oxford University Press, New York.

Ibers, J.A., and Hamilton, W.C. (1974) International tables for X-ray crystallography, vol. 4, p. 99–100. Kynoch Press, Birmingham, England.

Jeffery, J.W. (1952) The crystal structure of tricalcium silicate. Acta Crystallographica, 5, 26–35.

Kampf, A.R., and Moore, P.B. (1976) The crystal structure of bermanite, a hydrated manganese phosphate mineral. American Mineralogist, 61, 1241–1248.

Lovering, J.F., Wark, D.A., Reid, A.F., Ware, N.J., Keil, K., Prinz, M., Bunch, T.E., El Goresy, A., Ramdohr, P., Brown, G.M., Peckett, A., Phillips, R., Cameron, E.N., Douglas, J.A.V., and Plant, A.G. (1971) Tranquillityite: A new silicate mineral from Apollo 11 and Apollo 12 basaltic rocks. Proceedings of the Second Lunar Science Conference, vol. 1, p. 39–45. The M.I.T. Press, Boston, Massachusetts.

Magnusson, N.H. (1930) Långbans Malmtrakt: Geologisk Beskrivning. Sveriges Geologiska Undersökning, Ca, 23, Kungliga Boktrykeriet, Stockholm, 55–56.

Moore, P.B. (1970) Manganostibite: A novel cubic close-packed structure type. American Mineralogist, 55, 1489–1499.

——— (1989) Perception of structural complexity: Fillowite revisited and α-iron related. American Mineralogist, 74, 918–926.

Moore, P.B., and Araki, T. (1976) Braunite: Its structure and relationship to bixbyite, and some insights on the genealogy of fluorite derivative structures. American Mineralogist, 61, 1226–1240.

——— (1977) Mitridatite, $Ca_6(H_2O)_6[Fe^{3+}_9O_6(PO_4)_9]\cdot 3H_2O$, a noteworthy octahedral sheet structure. Inorganic Chemistry, 16, 1096–1106.

——— (1979) Armangite, a fluorite derivative structure. American Mineralogist, 64, 748–757.

O'Keeffe, M., and Hyde, B.G. (1985) An alternative approach to non-molecular crystal structures, with emphasis on the arrangements of cations. Structure and Bonding, 61, 77–144.

Pauling, L. (1929) The principles determining the structure of complex ionic crystals. Journal of the American Chemical Society, 51, 1010–1026.

——— (1960) The nature of the chemical bond (3rd edition), p. 505–562. Cornell University Press, Ithaca, New York.

Ramdohr, P., and Strunz, H. (1980) Klockmann's Lehrbuch der Mineralogie, 16 Auflage, p. 680. Ferdinand Enke Verlag, Stuttgart.

Rau, V.G., and Kurkutova, E.N. (1973) Crystal structure of långbanite. Soviet Physics Crystallography, 18, 320–322.

Shannon, R.D., and Prewitt, C.T. (1969) Effective ionic radii in oxides and fluorides. Acta Crystallographica, B25, 925–946.

Strunz, H. (1944) Abhandlungen. Wahrscheinliche Dimorphie zwischen Braunit und Långbanit. Neues Jahrbuch für Mineralogie Monatshefte 1944 Abt. A, 241–243.

Villars, P., and Calvert, L.D. (1985) Pearson's handbook of crystallographic data for intermetallic phases, vols. 1–3, 3258 p. American Society for Metals, Metals Park, Ohio.

Wells, A.F. (1975) Structural inorganic chemistry (4th edition), p. 136–140. Clarendon Press, Oxford, England.

Zachariasen, W.H. (1968) Experimental tests of the general formula for the integrated intensity of a real crystal. Acta Crystallographica, A24, 212–216.

Manuscript received September 14, 1990
Manuscript accepted April 9, 1991